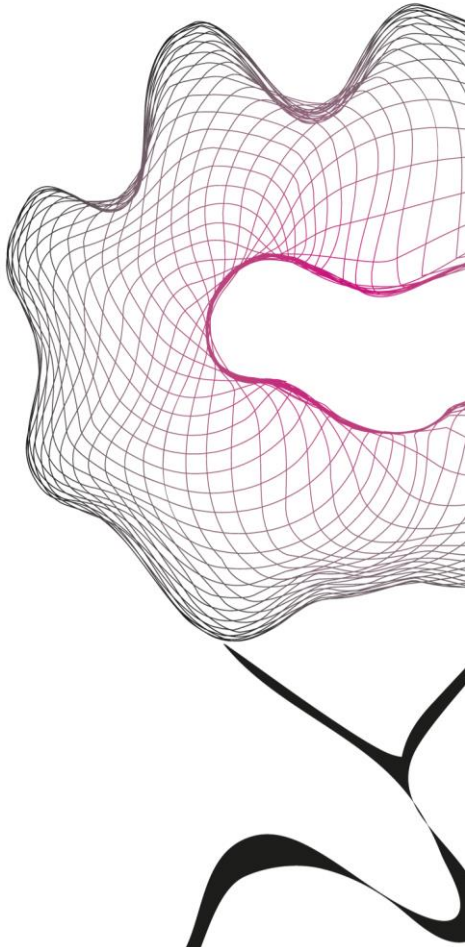


MASTER THESIS



VOLUMETRIC CAPNOGRAPHY AND CO/NO DIFFUSION TO EXCLUDE PULMONARY EMBOLISM AT THE EMERGENCY ROOM

T.M. Fabius

TECHNICAL MEDICINE – MEDICAL SENSING AND STIMULATION
FACULTY OF SCIENCE AND TECHNOLOGY

EXAMINATION COMMITTEE

Chair:	Prof. P.H. Veltink, PhD
Medical supervisor:	M.M.M. Eijsvogel, MD
Technical supervisor:	F.H.C. de Jongh, PhD
Mentor:	M. Groenier, PhD
External member:	E.J.F.M. ten Berge, MD, PhD
Extra member:	I. van der Lee, MD, PhD

Date: 20-08-2015

Abstract

Rationale: Literature has suggested the use of end-tidal P_{CO_2} (PET_{CO_2}) to exclude pulmonary embolism (PE). The analysis of the entire curve of the P_{CO_2} in expired air (volumetric capnography), which might indicate increased dead space, might result in a more specific exclusion tool for PE in addition to Wells-score and D-dimer. With its capability to indicate pulmonary vascular abnormalities, the ratio of the transfer factor of the lungs for nitric oxide and the transfer factor of the lungs for carbon monoxide ($T_{L,NO}/T_{L,CO}$) might also be a useful tool to rule out pulmonary embolism (PE).

Methods: CO/NO diffusion and volumetric capnography measurements were performed on subsequent patients seen on the emergency department for which due to suspected PE a computed tomography pulmonary angiogram (CTPA) was ordered.

Results: A total of 31 patients were included, PE was found on CTPA in 13 patients. Median $T_{L,NO}/T_{L,CO}$ ratio was 4.09 (IQR 3.83 - 4.40) in the no PE group versus 4.00 (IQR 3.78 - 4.32) in the PE group (p=0.959). Median alveolar volume was 77.1% of predicted (IQR 65.5 - 87.8) in the no PE group versus 71.0% of predicted (IQR 65.0 - 81.4) in the PE group (p=0.353). Median $T_{L,CO}$ was 75.8% of predicted (IQR 62.9 - 89.6) in the no PE group versus 68.8% of predicted (IQR 58.5 - 75.7) in the PE group (p=0.120). Median $T_{L,NO}$ was 69.3% of predicted (IQR 57.0 - 76.1) in the no PE group versus 60.5% of predicted (IQR 46.6 - 68.9) in the PE group (p=0.078). Median PET_{CO_2} was 4.37 kPa (IQR 4.00-4.83) in the no PE group versus 4.07 kPa (IQR 3.37-4.38) in the PE group (p=0.075). Median airway dead space was 2.68 mL/kg (IQR 2.32 - 3.07) in the no PE group versus 2.98 mL/kg (2.60 - 3.33) in the PE group (p=0.149). Median of a novel parameter consisting of several volumetric capnogram characteristics, $\frac{V_{CO_2} \times slope_{III}}{RR}$ (with V_{CO_2} being the amount of CO_2 exhaled per breath, $slope_{III}$ the slope of the alveolar phase of the volumetric capnogram and RR the respiratory rate), was 1.85 (IQR 1.21-3.00) in the no PE group versus 1.18 (0.61-1.38) in the PE group (p=0.006). Area under the curve (AUC) of the receiver operating characteristic (ROC) curve of PET_{CO_2} was 0.69 (95%CI 0.50-0.88 p=0.075). AUC of the ROC curve of the new parameter $\frac{V_{CO_2} \times slope_{III}}{RR}$ was 0.79 (95%CI 0.64 - 0.95 p=0.006). Using a threshold for the new parameter of 1.90 kPa.s/L or higher to exclude PE results in a negative predictive value of 100% with a positive predictive value of 54%.

Conclusion: The presented data indicate that the $T_{L,NO}/T_{L,CO}$ ratio and PET_{CO_2} alone cannot be used to exclude PE. The developed parameter $\frac{V_{CO_2} \times slope_{III}}{RR}$ shows more promising results.

Contents

Abstract	3
Table of abbreviations	7
1 Introduction	9
2 Background	11
2.1 Anatomy	11
2.2 Pulmonary Embolism	12
2.2.1 Pathophysiology	12
2.2.2 Diagnosis	12
2.2.3 Management	13
2.3 CO/NO Diffusion	16
2.3.1 Principle	16
2.3.2 Measurement	17
2.3.3 Applications	18
2.4 Volumetric Capnography	18
2.4.1 Principle	18
2.4.2 Applications	20
3 Methods	21
3.1 CO/NO diffusion	21
3.2 Volumetric capnography	22
3.2.1 Measurement	22
3.2.2 Analysis	22
3.2.3 New Parameter	23
3.3 Statistical Analysis	24
4 Results	25
4.1 CO/NO diffusion	25
4.2 Volumetric capnography	25
5 Discussion	29
5.1 Patient Characteristics	29
5.2 CO/NO diffusion	29
5.3 Volumetric capnography	32
6 Conclusion	35
7 Future Research and Recommendations	37

Acknowledgments	39
Bibliography	41
Appendix - Simulation model of the respiratory gas exchange	47
7.1 Respiratory control	48
7.2 Bicarbonate buffer	49
7.3 Simulation	50
7.4 Limitations	50

Table of abbreviations

<i>Abbreviation</i>	<i>Meaning</i>
AUC	Area under the curve
AVDSf	Alveolar dead space fraction
BMI	Body mass index
CI	Confidence interval
CO	Carbon monoxide
CO_2	Carbon dioxide
CTPA	Computed tomography pulmonary angiogram
Dm	Diffusion capacity of the alveolar-capillary membrane
K_{CO}	Transfer coefficient of the lungs for carbon monoxide
K_{NO}	Transfer coefficient of the lungs for nitric oxide
GUI	Graphical user interface
NO	Nitric oxide
NPV	Negative predictive value
Pa_{CO_2}	Arterial partial pressure of carbon dioxide
PE	Pulmonary embolism
PESI	Pulmonary embolism severity index
PET_{CO_2}	End-tidal partial pressure of carbon dioxide
PPV	Positive predictive value
ROC	Receiver operating characteristic
RR	Respiratory rate
$T_{L,CO}$	Transfer factor of the lungs for carbon monoxide
$T_{L,NO}$	Transfer factor of the lungs for nitric oxide
V_A	Alveolar volume
V_c	Pulmonary capillary blood volume
V_D	Dead space
VCO_2	Amount of carbon dioxide exhaled per breath
VDaw	Airway dead space
V/P scan	Ventilation/perfusion scan
V_T	Tidal volume
θ	Reaction rate of the binding of a gas with hemoglobin

Table 1: Table of abbreviations

Chapter 1

Introduction

Pulmonary embolism (PE) is a potentially lethal pathology which is hard to diagnose without expensive imaging techniques. Several tools to screen patients for PE, such as D-Dimer [1] and the Wells-score [2] exist. These tests can safely rule out PE but cannot be used to confirm it [3]. The golden standard for confirming PE is a computed tomography pulmonary angiogram (CTPA) [4]. When one of the screening modalities indicates the possible presence of PE, a CTPA needs to be made to confirm the diagnosis. Due to the low specificity of the screening modalities many CTPAs (up to 75%) rule out PE [4]. Moreover, in order to make a CTPA the patient needs to be infused with a contrast medium. Patients with poor kidney function have to be prehydrated before the contrast can be applied safely making admission to the ward in most cases inevitable. Therefore, the search to a fast, cheap and easily applied screening method for PE continues.

In 1959, the end-tidal partial carbon dioxide pressure (PET_{CO_2}) has been suggested as possible screening tool for PE several times [5]. The rationale behind this parameter is that PE increases functional dead space and therefore decreases the fraction CO_2 in exhaled air. Due to technical limitations, the use of capnography in PE was abandoned. However, improvement of the measurement techniques renewed the use of this promising parameter. Several studies on PET_{CO_2} in suspected PE patients have been performed since. Most of the studies reported a significant lower PET_{CO_2} in patients with PE compared to patients without PE. However, there are many other pathologies which may result in a lowered PET_{CO_2} . This led to the development of volumetric capnography which allows analysis of the entire curve of the expired CO_2 . Using this, parameters such as (functional) dead space can be calculated. In a meta-analysis of 14 studies Manara et al. concluded that (volumetric) capnography might be used to exclude PE in patients with a pretest probability less than 10% [6]. However, almost all studies reviewed by Manara et al. only investigated the end tidal alveolar dead space fraction (AVDSf), i.e. a quantification of the difference in PET_{CO_2} and arterial P_{CO_2} (Pa_{CO_2}). We believe that using more characteristics of the total volumetric capnogram (such as the slope of the alveolar phase) might add substantial value to the screening capabilities of volumetric capnography.

Though several characteristics of the volumetric capnogram might safely rule out PE, it might not enable the confirmation of PE. Therefore an additional diagnostic modality is needed. We hypothesized that a CO/NO-diffusion test might allow for a differentiation in hemodynamic or pulmonary origin of the aberrant volumetric capnogram. In the CO/NO-diffusion test the transfer factors for carbon monoxide ($T_{L,CO}$) and nitric oxide ($T_{L,NO}$) are determined. Following the Roughton-Fourster equation, the transfer factor for a specific gas is dependent on how easily it can diffuse over the alveolar-capillary membrane and how easily it can bind to hemoglobin. NO binds much faster to hemoglobin compared with CO. $T_{L,NO}$ is therefore mainly dependent on the membrane component whereas $T_{L,CO}$ is dependent on both the membrane and hemodynamic component. Theoretically, if the ratio of $T_{L,NO}$ and $T_{L,CO}$ is calculated, some information on the

hemodynamic component (which should be aberrant in PE) should be obtained. This principle was investigated by van der Lee and Hughes who did find aberrant $T_{L,NO}/T_{L,CO}$ ratios in pathologies with a hemodynamic component such as pulmonary hypertension [7,8]. Harris et al. showed an increased $T_{L,NO}/T_{L,CO}$ ratio after pulmonary artery obstruction in sheep. [9] To our knowledge, the $T_{L,NO}/T_{L,CO}$ ratio during PE has not been investigated in humans.

Chapter 2

Background

2.1 Anatomy

The lungs consist of five lobes; three in the right lung (upper, middle and lower) and two in the left lung (upper and lower). Each lobe in turn consists of several segments. Each segment consists of several subsegmental parts, and so on until the terminal segments are reached, consisting of alveoli. Gas exchange takes place in these alveoli, all other parts of the respiratory system are conducting airways. In order to enable gas exchange in the alveoli they need to be ventilated and perfused. An overview of the pulmonary vasculature is provided in figure 2.1. Deoxygenated blood travels from the periphery through the vena cava to the right atrium of the heart, to the right ventricle and is then pumped into the pulmonary artery. The pulmonary artery divides into the right and left pulmonary artery which again divide into lobar, segmental and subsegmental arteries until they arrive at the alveoli where they transcend into capillaries where the gas exchange takes place. The oxygenated blood in the pulmonary capillaries flows into the subsegmental veins which merge into the segmental, lobar and ultimately main pulmonary vein. From the pulmonary vein, the blood flows into the left atrium, then the left ventricle where the heart pumps into the aorta on its way to the organs to deliver the oxygen and absorb carbon dioxide. [10]

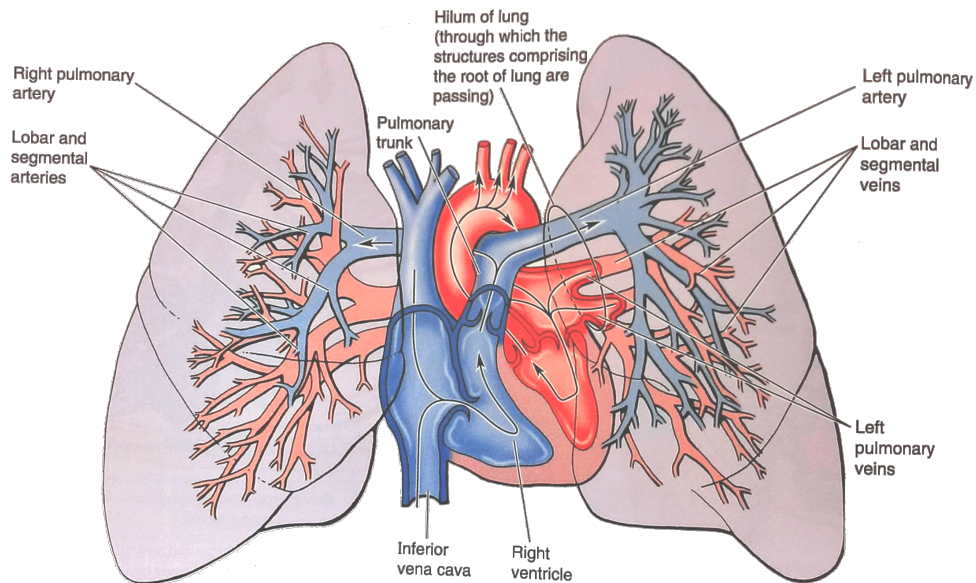


Figure 2.1: Overview of the pulmonary circulation. Copied from Moore et al. [10].

2.2 Pulmonary Embolism

2.2.1 Pathophysiology

A pulmonary embolus is defined as a particle which (partially) obstructs the arteries of the lungs. In most cases this particle is a thrombus (blood clot), originating from the deep peripheral veins located in the legs. The thrombi often form due to prolonged inactivity such as immobilization after surgery or long travels. Other particles causing pulmonary embolism are fat particles, air (or other gases) bubbles, tumor cells, etc. The consequences of the obstruction of the pulmonary arteries can vary from none to mild dyspnea and chest pain to infarction of the lung tissue and sudden death. After the obstruction of (a part of) the pulmonary artery, a part of the affected lung is ventilated but not perfused (i.e. dead space ventilation). This causes a limitation in the gas exchange. As the body still produces the same amount of CO_2 and needs the same amount of O_2 , ventilation of the healthy parts of the lungs needs to increase. The amount of increase in ventilation is dependent on the amount of alveoli affected by the emboli. Massive central pulmonary embolism, i.e. multiple clots obstructing the main branches of the pulmonary artery, are likely to cause severe symptoms as they cause a large obstruction. A small single embolus obstructing a subsegmental artery is far less likely to cause substantial problems. This is partly because only a small part of the lung suffers from the obstruction. But also because the small obstruction does not cause a significant rise in pressure in the pulmonary arteries (i.e. there is no pulmonary hypertension). A large central thrombus will cause a significant rise in pressure, as the same amount of blood has a opening to pass through. This rise in pressure (or resistance) can cause right ventricle failure, leading to a decrease in cardiac output and eventually death. If an obstruction completely blocks the blood flow to the lung tissue, infarction of this tissue can occur. However, this does not happen often as lung tissue also receives blood from the bronchial arteries. If emboli obstruct a part of the vasculature for a prolonged period of time, chronic pulmonary embolism can occur which often leads to chronic thromboembolic pulmonary hypertension. Next to the increased resistance the right ventricle has to overcome, the increased pressure in the pulmonary arteries also leads to changes in the walls of the affected vessel which impair gas exchange. [11]

2.2.2 Diagnosis

Depending to the extent of the pulmonary embolism, it is fatal in 1-60 % of the cases. In many cases it does not cause any symptoms and post-mortem autopsies have shown the presence of emboli in up to 60% of all cases. Even in hemodynamic stable patients, mortality rates up to 15% have been reported. [12] Therefore, PE needs to be ruled out with high certainty (or confirmed) when suspected. Due to the aspecificity of the symptoms of PE (dyspnea, chest pain, tachypnea), PE can be suspected in many cases. An often used first diagnostic step is the determination of the D-dimer level. A D-dimer level of less than 500 $\mu\text{g/L}$ safely excludes PE [1].

As many other pathologies can cause elevated D-dimer levels, it should only be determined when the presence of PE is likely. To determine this several clinical suspicion scoring system exist. The most used scoring systems are the Geneva and Wells scores of which the Wells-score is most used in the Netherlands. An overview of this scoring system is provided in table 2.1. The Wells-score classifies the presence of PE as unlikely or likely (of which 'PE likely' obviously warrants further investigation) [2]. Though current guidelines state that D-dimer should not be evaluated without increased suspicion of PE [13], it is often determined concurrently with the clinical suspicion creating a dilemma when the Wells-score rules out PE and the D-dimer level is elevated (which warrants further investigation).

Many disorders can cause the Wells-score and D-dimer levels to be raised. Therefore PE is excluded in the majority (up to 75%) of the CTPAs [4]. To decrease this number, a new D-dimer level

Table 2.1: The Wells-score used to classify the suspicion on pulmonary embolism [2]. DVT denotes deep vein thrombosis, PE denotes pulmonary embolism.

<i>Variable</i>	<i>Points</i>
Clinical signs and symptoms of DVT	3.0
PE most likely diagnosis	3.0
Hear rate higher than 100/min	1.5
Immobilization or surgery in last four weeks	1.5
Previous DVT or PE	1.5
Hemoptysis	1.0
Malignancy (active or in last six months)	1.0
<i>Clinical probability</i>	<i>Total score</i>
PE unlikely	≤ 4
PE likely	> 4

threshold dependent to age has been proposed [14]. Though this cut-off value strongly increases the number of cases in which PE can safely be ruled out, PE can still not be ruled out in over 70% of the patients without PE.

The next step in the exclusion or confirmation of PE is some form of imaging technique. If there are signs of deep venous thrombosis (DVT) an ultrasound of the legs can be made to confirm its presence. As the presence of respiratory symptoms combined with DVT is almost synonymous with the presence of PE, and the treatment of PE and DVT are similar, no further investigations are needed when DVT is shown on ultrasound [13]. If there are no signs of DVT or DVT is not seen on ultrasound, either a CTPA or ventilation/perfusion scan (V/P-scan) needs to be made. Due to its high resolution, CTPA is preferred. In CTPA, a contrast medium is injected into the veins and a series of X-ray images is made when the contrast medium reaches the pulmonary artery. If PE is present, contrast defects will be visible on the resulting images (see figure 2.2a). The advantage of the CTPA is its high spatial resolution, i.e. even small emboli can be visualized. Its disadvantage is that potentially harmful X-rays and contrast medium are needed. In a V/P scan, first a radioactive substance is injected into the veins and radioactivity of the body is measured after a small time allowing quantification of the lung perfusion. Subsequently, a radioactive substance is inhaled and again the radioactivity of the body is measured allowing quantification of lung ventilation. In the presence of PE, typically a part of the lung is ventilated but not perfused (see figure 2.2b). The advantage of the V/P scan is that the amount of perfusion defect can be quantified (i.e. the part of the lung that does not receive perfusion). However, it has a low resolution and may not detect subsegmental or non-occluding emboli as these do not always cause significant perfusion defects. [15]

2.2.3 Management

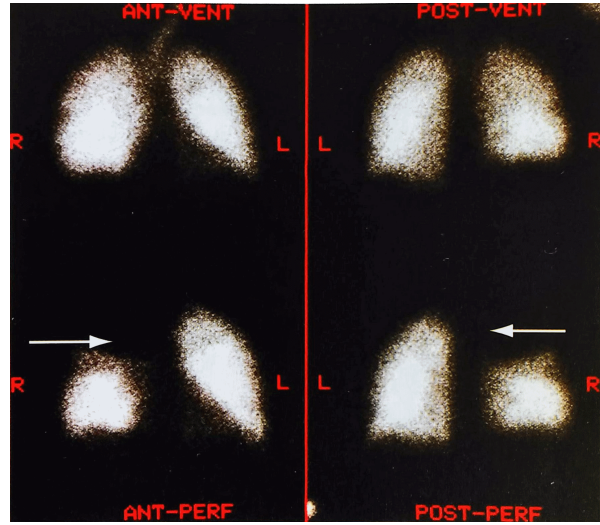
Flow chart of the 2014 ESC/ERS guidelines on the management of pulmonary embolism is provided in figure 2.3. In this figure it can be seen that the presence of shock or hypotension in PE warrants primary reperfusion, i.e. the thrombus/thrombi need to be dissolved quickly requiring intervention (thrombolysis).

If there is no shock or hypotension, further risk stratification is needed. To do so, the pulmonary embolism severity index (PESI) has been developed [17]. This index uses several clinical parameters to divide the risk on adverse outcome in five classes. An overview of the PESI is given in table 2.2. If the outcome of PESI is class III to V, the right ventricular function needs to be

Figure 2.2: Examples of a CTPA and V/P scan, both showing the presence of pulmonary embolism.



(a) Example of a computed tomographic pulmonary angiogram (CTPA) showing a massive pulmonary embolus in the right pulmonary artery indicated by the black arrow. Copied from Kumar and Clark [11].



(b) Example of a ventilation/perfusion scan (V/P scan) showing the probable presence of pulmonary embolism in the right upper lobe indicated by the presence of ventilation and lack of perfusion (white arrows). Copied from Kumar and Clark [11].

Table 2.2: The pulmonary embolism severity index (PESI) used to classify the risk on adverse outcome in pulmonary embolism [17].

<i>Variable</i>	<i>Points</i>
Age (years)	1/year
Male sex	10
Cancer (history or active)	30
Heart failure (history or active)	10
Chronic lung disease (history or active)	10
Heart rate ≥ 110 /min	20
Systolic blood pressure < 100 mmHg	30
Respiratory rate ≥ 30 /min	20
Temperature < 36 °C	20
Altered mental status	60
Oxygen saturation $< 90\%$	20
<i>Risk stratification</i>	<i>Total score</i>
Class I - very low risk	≤ 65
Class II - low risk	66-85
Class III - intermediate risk	86-105
Class IV - high risk	106-125
Class V - very high risk	> 125

assessed using imaging techniques and laboratory testing (e.g. troponin or NT-proBNP). In the case that both laboratory tests and imaging techniques indicate cardiac dysfunction, the risk is

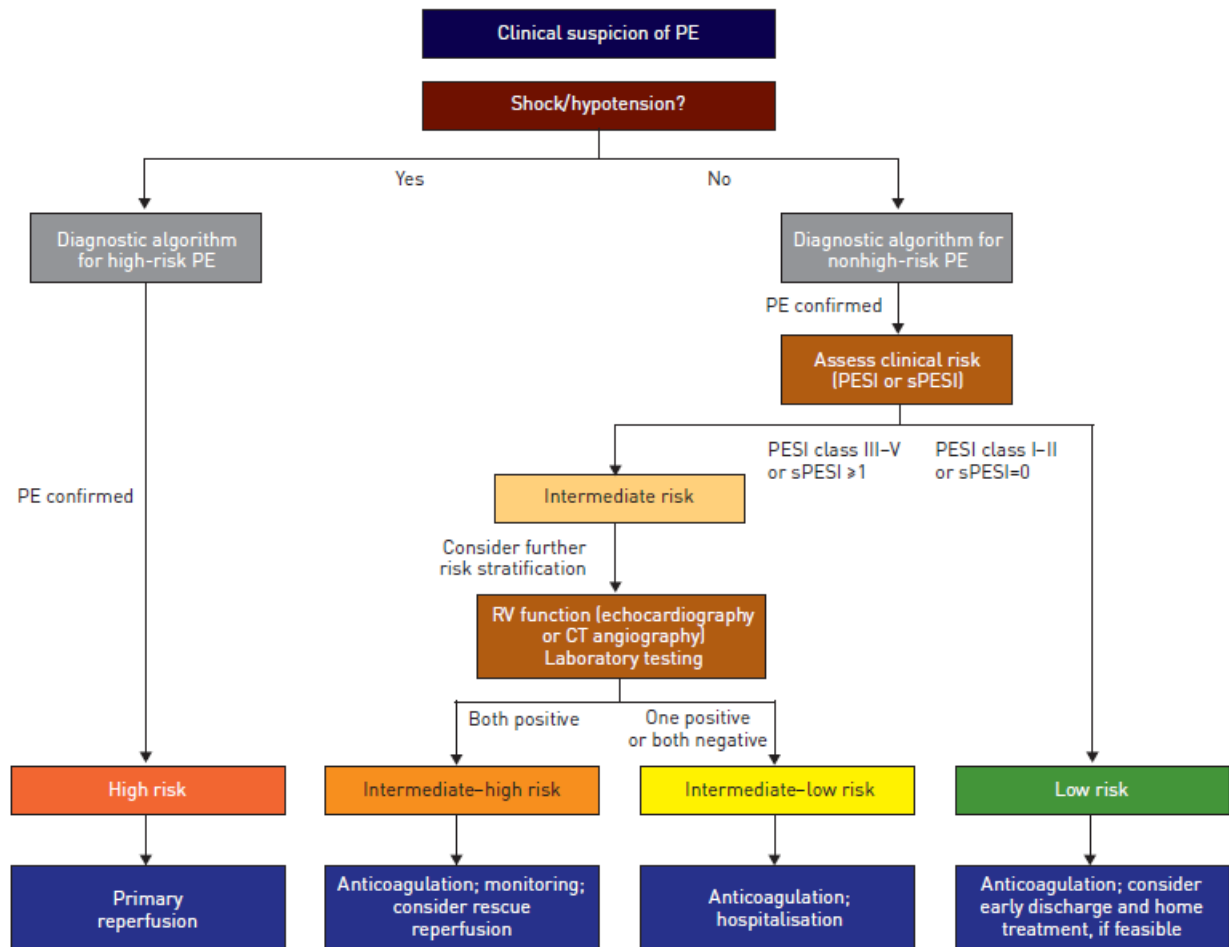


Figure 2.3: Flow chart of the 2014 ESC/ERS guidelines on the management of pulmonary embolism. Copied from Konstantinides et al. [16].

stratified as intermediate high risk in which reperfusion by thrombolysis still might be necessary next to anticoagulation. Otherwise, it is stratified as intermediate low risk and conventional anticoagulation therapy is sufficient. In the case of PESI class I-II, the risk on adverse outcome is low and anticoagulation therapy is sufficient and the patient may even be sent home. To be able to select which low-risk patients need to be admitted and which can be sent home with treatment, the Hestia criteria can be used [18] (see table 2.3). The duration of anticoagulation treatment is dependent on the cause of the embolism. If a provocative process can be identified (e.g. surgery or immobilization), treatment is indicated for three months. In the case of idiopathic PE (i.e. no provocative process can be identified), treatment needs to be continued at least six months. In the case of recurrent PE within one year after cessation of anticoagulation treatment, treatment needs to be restarted and continued indefinitely. [16]

Table 2.3: The Hestia criteria for treatment at home. If the answer to all of the stated questions is 'No', the patient can safely be treated at home. Copied from Zondag et al. [19].

- Is the patient hemodynamically unstable?
- Is thrombolysis or embolectomy necessary?
- Active bleeding or high risk of bleeding?
- More than 24 h of oxygen supply to maintain oxygen saturation > 90%?
- Is PE diagnosed during anticoagulant treatment?
- Severe pain needing intravenous pain medication for more than 24 h?
- Medical or social reason for treatment in the hospital for more than 24 h?
- Does the patient have a creatinine clearance of < 30 mL/min?
- Does the patient have severe liver impairment?
- Is the patient pregnant?
- Does the patient have a documented history of heparin-induced thrombocytopenia?

2.3 CO/NO Diffusion

2.3.1 Principle

Gas exchange is a continuous process exclusively driven by passive diffusion. The amount of a gas which will cross the alveolar-capillary membrane per time unit is given by a simplified version of Ficks law:

$$\dot{V}_{net} = T_L(P_A - P_c) \quad (2.1)$$

in which \dot{V}_{net} denotes the amount of gas that will cross the alveolar-capillary membrane per minute, T_L denotes the transfer factor of the lungs in mL (or mmol)/min/kPa, P_A denotes the partial pressure of the gas in the alveolar space and P_c denotes the partial pressure of the gas in the pulmonary capillaries. The first work on the transfer factor has been performed by Marie Krogh in the start of the 20th century. In those times, it was believed that oxygen was secreted actively in the lungs. Krogh discovered that alveolar P_{O_2} was always larger than arterial P_{O_2} and so the idea of passive diffusion was introduced. The transfer factor of the lungs for a certain gas describes the rate of uptake of the gas per time unit and pressure difference (hence its unit mmol/min/kPa). Krogh realized that the transfer factor is highly influenced by the alveolar volume (V_A), as a higher alveolar volume provides a greater surface over which the gas can diffuse. Therefore, she introduced the transfer coefficient (or Krogh-factor) K with unit mmol/min/kPa/L which corrects for alveolar volume. The definition of K is provided in equation 2.2. [20,21]

$$K = \frac{T_L}{V_A} \quad (2.2)$$

T_L (or D_L) is dependent the diffusion capacity of the membrane (D_m) and the binding of the gas on red blood cells. As gas passing from the lungs into the capillaries (or vice versa) passes several cell layers, D_m consists of multiple diffusion capacities. Or more precise, it is the reciprocate sum of these diffusion capacities. The binding to blood cells can be quantified as the affinity of the gas with red blood cells (θ , i.e. how many gas binds to hemoglobin during one minute per kPa (or mmHg) pressure difference) multiplied with the amount of blood present in the capillaries (V_c). Combining these factors results in the Roughton Forster equation [22] which is provided in equation 2.3.

$$\frac{1}{T_L} = \frac{1}{D_m} + \frac{1}{\theta V_c} \quad (2.3)$$

If one wants to measure T_L in physiologic conditions using the amount of gas that has diffused from the lungs into the capillaries or vice versa, a problem arises. As stated in equation 2.1, the

partial pressures of the gas in both the alveolar space and the capillaries needs to be known. As for all gases normally exchanged in the lungs, these partial pressures are not known at the same time. Therefore, carbon monoxide (CO) is used. CO is normally not present (in a substantial amount) in the air (and human body). Therefore, in a physiologic situation the partial pressure of CO in both the capillaries ($P_{c,CO}$) and the alveoli ($P_{A,CO}$) is zero. If a known volume of CO is inspired, and the volume of the alveolar space is known, one can measure the fraction of expired CO and thereby calculate the amount of CO that diffused into the capillaries and subsequently $T_{L,CO}$ as (due to the great affinity of CO to bind to Hb) $P_{c,CO}$ remains negligible.

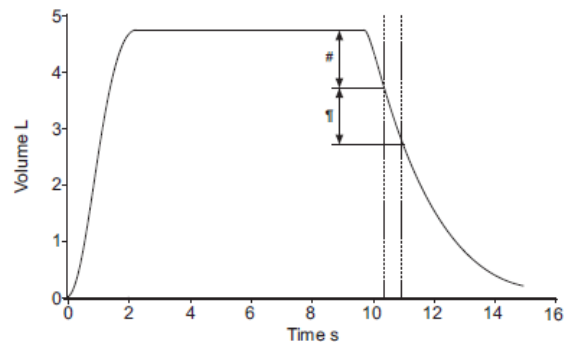
For $T_{L,CO}$, D_m and θV_c are approximately equal [22]. The binding capacity of NO to hemoglobin however, is much larger than the binding capacity of CO to hemoglobin [23]. Therefore, the second part of the equation ($\frac{1}{\theta V_c}$) can be ignored for NO, providing: $T_{L,NO} = D_{m,NO}$. Assuming that $D_{m,NO} = \alpha D_{m,CO}$, the $T_{L,NO}/T_{L,CO}$ ratio approaches $\alpha(1 + \frac{D_{m,CO}}{\theta_{CO} V_c})$. Thus, the $T_{L,NO}/T_{L,CO}$ ratio provides a measure for the D_m/V_c ratio without the need of estimating the value of θ (about which a lot of debate exists). [8]

2.3.2 Measurement

The measurement of diffusion capacity is mostly performed using the single breath technique. In this method, the subject inhales a gas mixture, holds his breath for several seconds and subsequently exhales completely. A sample of the exhaled air is analyzed to obtain the exhaled fractions of the tracer gas (in our case helium) and the diffused gases (CO and NO). As no diffusion takes place in the conducting airways, the first amount of exhaled air (usually approximately 600-700 mL) is discarded. The subsequent exhaled volume (often the same volume as the discarded volume is used) is used as sample of alveolar air. The air from this sample is analyzed. An overview of the inspired volume manoeuvre and measurement setup is provided in figure 2.4. [24] The amount of exhaled CO can be analyzed using fast sensors. Fast sensors also exist for NO but are rarely



(a) Setup of the single breath CO/NO diffusion measurement. The subject is attached to the Jaeger MasterScreen system via a mouthpiece and performs the measurement manoeuvre as displayed in (b). After the final exhalation, the gases in the bag are analyzed to be able to calculate $T_{L,CO}$, $T_{L,NO}$ and V_A .



(b) Measurement manoeuvre used in the single breath determination of $T_{L,CO}$ and $T_{L,NO}$. The subject first exhales completely. Then the patient inhales completely in which a gas admixture is inhaled, holds his breath for several seconds and subsequently exhales completely. The first exhaled air is discarded (depicted as #) a following fixed volume is used for analysis (depicted as ‡). Adapted from MacIntyre et al. [24].

Figure 2.4: Overview of the single-breath diffusion capacity measurement setup and manoeuvre.

used due to high costs and low reliability in the wide adapted diffusion measurement systems (e.g. the MasterScreen™ PFT Pro system). To allow the analysis of the exhaled NO fraction, the

alveolar sample is directed into a bag of which the air is slowly analyzed (analysis time of over one minute). After establishing the exhaled fraction of the gas, T_L is calculated using the formula depicted in equation 2.4 in which b denotes a conversion factor dependent on the used unities, V_A the measured alveolar volume, t the duration of breath hold, P_B the barometric pressure, P_{H_2O} the vapor pressure of water, F_o the fraction of the measured gas in the alveoli at the start of breath hold and F_{ex} the fraction of the measured gas in the alveoli at the end of breath hold (i.e. the measured exhaled fraction).

$$T_L = b \times \frac{V_A}{t \times (P_B - P_{H_2O})} \times \ln\left(\frac{F_o}{F_{ex}}\right) \quad (2.4)$$

F_o is not equal to the inspired fraction as the lungs still contain some air after complete exhalation. Therefore F_o is calculated using the inspired and expired fractions of tracer gas (which are a measure for alveolar volume). From equation 2.4 it can be seen that actually not the transfer factor but the transfer coefficient is measured, after which is multiplied with V_A to obtain T_L .

The volume of the alveolar space can be measured by the inspiration of an inert gas (i.e. a gas that cannot cross the alveolar-capillary membrane). If the fraction of expired gas is measured after a substantial time (long enough to let the inert gas distribute equal through the alveolar space) the alveolar volume can be calculated using equation 2.5, in which F_{ex} denotes the exhaled fraction of the inert gas, F_{in} denotes the inhaled fraction of the inert gas, V_{in} denotes the inspired volume, V_A denotes the alveolar volume and V_D the volume of the conducting airways (in which no gas exchange takes place, its volume is estimated based on height and weight).

$$V_A = \frac{F_{in} \times V_{in}}{F_{ex}} - V_D \quad (2.5)$$

In reality, corrections for the temperature and P_{CO_2} need to be made but equation 2.5 approximates the real value of V_A . [25]

2.3.3 Applications

The use of $T_{L,CO}$ is widely adopted in respiratory medicine. Combined with K_{CO} it is used to distinguish between loss of lung volume (in restrictive diseases such as a pneumothorax) and loss of functional lung tissue (in diseases affecting the alveolar-capillary membrane such as emphysema and fibrosis). A low $T_{L,CO}$ with a high K_{CO} indicates loss of volume, whereas if both $T_{L,CO}$ and K_{CO} are lowered, loss of function is indicated. Decreased $T_{L,CO}$ is amongst others seen in fibrosis, vasculitis, emphysema and pulmonary edema. [25] The use of $T_{L,NO}$ has not been adopted as routine diagnostic measure yet. Its application has mainly been in the research field. The $T_{L,NO}/T_{L,CO}$ ratio has been shown to be increased in heavy smokers [26], chronic thromboembolic pulmonary hypertension, diffuse parenchymal lung disease [7] and during acute PE in sheep [9] but is mainly used in research to quantify the capillary blood volume (V_c) and membrane diffusing capacity (D_m).

2.4 Volumetric Capnography

2.4.1 Principle

Capnography is the measurement of CO_2 . In medicine, it is mostly used to measure the fraction (or partial pressure) of exhaled air consisting of CO_2 (respectively F_{e,CO_2} and P_{e,CO_2}). Two measurement principles can be used, sidestream and mainstream. In a sidestream capnograph, a sample of the exhaled air is analyzed. In a mainstream capnograph, the sensor is located directly

on the breathing path, i.e. all exhaled air is analyzed. These sensors usually use fast infrared-spectroscopy measurements. This measurement principle uses the absorbance spectrum of CO_2 (i.e. the wavelengths of infrared light that is absorbed by CO_2) to quantify the amount of CO_2 . The main advantage of mainstream over sidestream is that mainstream allows for simultaneous flow measurements as the sensor is located direct on the breathing path. Using this allows for a plot of the exhaled P_{CO_2} as a function of the total exhaled volume. This results in a figure as provided in figure 2.5. Many developments in the (volumetric) capnography have been established by Roger

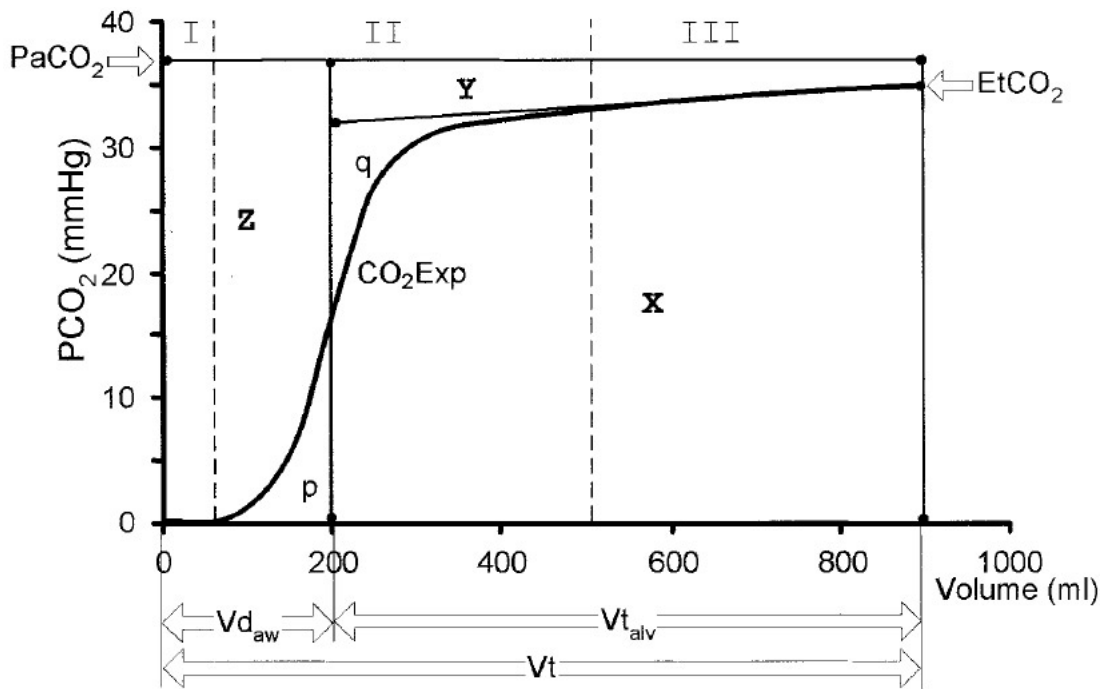


Figure 2.5: Example of a volumetric capnogram. Copied from Verschuren et al. [27].

Fletcher. He developed the "single breath test for carbon dioxide", a term which has lost its use over the years. Though several aspects of capnography were already investigated, Fletcher made its use more common practice in anesthesia. The capnogram allows for the derivation of several physiologic properties. First, the end-tidal P_{CO_2} (P_{ETCO_2} , the P_{CO_2} at the end of exhalation) is believed to be a good measure for the arterial P_{CO_2} (P_{aCO_2}) when no respiratory pathology is present. Second, the volume of exhaled CO_2 can be calculated relatively simple as the area under the curve. Another application is the determination of the volume of airway dead space. As can be seen in figure 2.5, the capnogram consists of three phases. The first (phase I) consists solely of air from the conducting airways and therefore contains no CO_2 . The second phase (phase II), consists of a mixture of air from conducting airways and alveolar air, therefore a transient rising level of CO_2 is noticed. The last phase (phase III) consists purely of alveolar air, showing a linear rising level of CO_2 as diffusion of CO_2 continues to take place during exhalation. If a linear approximation of phase III is created (line Y in figure 2.5), the volume of airway dead space can be determined by drawing a vertical line at the volume where the area between the vertical line, the capnogram and the x-axis (area p in figure 2.5) is equal to the area between the vertical line, the capnogram and the linear approximation of phase III (area q in figure 2.5). This method to determine the conducting airway dead space is called the equal-area method and has been described first by Fowler et al. [28]. [29]

If the P_{aCO_2} is also known, physiologic dead space can also be determined. This method has

been developed first by Christian Bohr who proposed the Bohr dead space equation as depicted in equation 2.6 in which V_D depicts the total amount of dead space, V_T the tidal volume, F_{A,CO_2} the alveolar fraction of CO_2 and F_{E,CO_2} the mixed expired fraction of CO_2 (i.e. the average expired fraction CO_2) [30].

$$\frac{V_D}{V_T} = \frac{F_{A,CO_2} - F_{E,CO_2}}{F_{A,CO_2}} \quad (2.6)$$

F_{A,CO_2} was determined as the measured F_{CO_2} in late exhalation. However, approximately 40 years later it was recognized that a difference in arterial and alveolar P_{CO_2} can exist making Bohr's formula providing misleading low amounts of dead space. Therefore, Enghoff modified Bohr's formula by substituting F_{A,CO_2} by the arterial P_{CO_2} (P_{aCO_2}) (and F_{E,CO_2} by P_{E,CO_2}) as depicted in equation 2.7 [31].

$$\frac{V_D}{V_T} = \frac{P_{aCO_2} - P_{E,CO_2}}{P_{aCO_2}} \quad (2.7)$$

This equation is called the Bohr-Enghoff equation and is still used to calculate physiologic (the sum of anatomic and alveolar dead space) dead space. [32]

2.4.2 Applications

As said earlier, capnography is mainly used in anesthesia to monitor respiratory status intra-operatively or in the intensive care unit. Consequently, research using volumetric capnography has focused on this fields. In recent years, many research on the volumetric capnogram has been performed by the group of Tusman et al. They validated the calculation of Bohr dead space using volumetric capnography [33]. Kallet et al. used capnography to quantify the amount of dead space during acute respiratory distress syndrome [34]. Böhm et al. investigated the use of the slope of phase III to detect the amount of lung recruitment during the increase of positive end-expiratory pressure in mechanically ventilated patients [35].

The use of capnography to detect PE has first been pitched by Robin et al. in 1959 [5]. However, the existing techniques to measure P_{CO_2} had too many drawbacks mostly concerning the large number of false positives (no golden standard imaging technique was available at the time, capnography was proposed as the standard technique to confirm PE), as described by Nutter and Massum in 1966 [36]. Therefore, the use of capnography to detect PE was abandoned. In the mid 90's however, techniques had evolved and interest to exclude PE rather than confirm it renewed [37]. Research mainly investigated the use of the alveolar dead space fraction (AVDSf) to exclude or confirm PE (e.g. [38–41]). The AVDSf is a modified form of the Bohr-Enghoff formula in which P_{E,CO_2} is replaced by the end-tidal P_{CO_2} (P_{ETCO_2}). In 2013 however, Manara et al. show in an extensive meta-analysis that the use of AVDSf has little added value to the current diagnostic capabilities in PE [6]. The use of several volumetric capnogram characteristics during PE in spontaneously breathing patients has only been investigated by the group of Verschuren et al. [27]. They also published reference values for several characteristics in healthy spontaneously breathing subjects [42] which were unknown until then due to the almost exclusive use of capnography in ventilated patients.

Next to the use of the AVDSf, the P_{ETCO_2} alone has also been investigated to exclude PE. These studies all reported that a P_{ETCO_2} above a certain threshold safely excludes the presence of PE. Rumpf et al. reported a threshold of 28 mmHg (3,7 kPa) [43], Hemnes et al. a threshold of 36 mmHg (4.8 kPa) [44] and Riaz and Jacob a threshold of 4.3 kPa [45]. Needless to say, the validation of such a threshold is essential. No such studies have been performed yet.

Chapter 3

Methods

Patients (age at least 18 years) seen at the emergency room of the Medisch Spectrum Twente, seen by a pulmonologist for which due to suspected PE a CTPA was requested, were included in the study. Exclusion criteria were:

- Hemodynamic instability; Measurements were performed on the pulmonary function department, so the patient had to be able to leave the emergency room safely.
- Pregnancy; Pregnancy can influence arterial CO_2 levels [46] and therefore might influence the volumetric capnography measurements. Ethical arguments were also a reason to exclude pregnant women.
- Oxygen administration; Altered alveolar oxygen levels directly influence the diffusion capacity of the lungs [47]. Therefore, the ERS guidelines of singlebreath $T_{L,CO}$ measurement discourage the measurement of $T_{L,CO}$ during oxygen administration [24]. Though temporarily removal of the oxygen administration is medically possible in most cases, this is burdensome for the patient and was not covered by the consent of the local ethics committee to this study.

After obtaining informed consent, relevant clinical values (Hemoglobin level (Hb), D-dimer value and Wells-score) were recorded and the patient was taken to the pulmonary function department to perform the measurements within four hours of the request of the CTPA (and before the results were reported to the pulmonologist).

3.1 CO/NO diffusion

The CO/NO diffusion measurements were performed according the 2005 ATS/ERS guidelines on the single-breath measurement of $T_{L,CO}$ [24] using the MasterScreen™ PFT Pro system¹ (as described earlier in section 2.3.2). According to the ATS/ERS guidelines, a measurement was considered repeatable when the results of at least two tests were within 10% of the highest resulting values for $T_{L,CO}$ and $T_{L,NO}$ and the inspired volume of the most recent measurement was not the greatest. A maximum of five measurements were performed with at least four minutes between two tests. The reproduced measurements are saved on a local server and printed.

Predicted values of the CO-diffusion parameters, alveolar volume and vital capacity are provided by LabManager, the software of the MasterScreen™ PFT Pro system. Predicted values for $T_{L,NO}$ are calculated using the reference equations of van der Lee et al. [48]. Absolute values and its value compared to predicted of $T_{L,CO}$, K_{CO} , VA, inspired volume and $T_{L,NO}$ are stored for statistical analysis.

¹CareFusion, Amsterdam, the Netherlands

3.2 Volumetric capnography

The volumetric capnogram was recorded in the waiting time between the first and second CO/NO diffusion measurement using a Novametrix Co2smoPlus mainstream capnograph².

3.2.1 Measurement

The patient was asked to breath normally via a mouthpiece connected to the mainstream capnograph, with nostrils clipped. Every approximate two minutes, the data was saved and analyzed using a custom script in Matlab³ to assess its usability. Recording of the volumetric capnogram was stopped when at least two usable recordings were saved.

3.2.2 Analysis

The exported data consisted of the capnograph flow and P_{CO_2} data which were recorded with a sampling frequency of 100 Hz. Flow and CO_2 data were filtered with a low-pass filter using a cutoff frequency of 1 Hz to smooth the signals and remove artefacts. To determine the starting points of in- and expirations the sign of the flow data (positive (1) or negative (-1)) was calculated. Where the sign of the flow data changed from -1 to 1, an inspiration started. Where it changed from 1 to -1, an expiration started.

Assessment of usability With the starting and ending point of each expiration known each exhalation was examined on artifacts. If an exhalation consisted of less than 10 mL, contained a maximal P_{CO_2} of less than 0.5 kPa, took less than 0.1 seconds or contained a decline in P_{CO_2} of more than 10 kPa/s the expiration was excluded from analysis. All of these thresholds are chosen very conservatively to allow a wide variety of expirations.

Hereafter the combined z-score of tidal volume (V_T), PET_{CO_2} and expiratory time (t) were calculated. The definition of the z-score is provided in eq 3.1 where X is the local value of the given set of values, μ is the mean the given set of values and σ its standard deviation.

$$Z = \frac{X - \mu}{\sigma} \quad (3.1)$$

To obtain the most similar set of exhalations as possible, the exhalation with the largest combined z-score is excluded from analysis until the 10 most equal exhalations are left for analysis.

A final check was performed using a method reported by Verschuren et al, i.e. the calculation of the coefficient of variation [27]. The definition of the coefficient of variation C is given in eq 3.2 where again μ is the mean of a given set of values and σ its standard deviation.

$$C = \frac{\sigma}{\mu} \quad (3.2)$$

The coefficient of variation of V_T (C_{VT}), PET_{CO_2} (C_{PETCO_2}) and t (C_t) were calculated. In accordance with Verschuren et al., the expirations were approved for further analysis if C_{VT} and C_t were below 0.2 and C_{PETCO_2} below 0.05.

²Co2smo Plus! 8100, Novametrix Medical Systems Inc, now Philips Respironics Inc., Murrysville, Pennsylvania, USA

³Matlab R2014a, The MathWorks Inc., Natick, Massachusetts, USA

Determination of parameters If the expirations are usable for further analysis, the starting points of phase II and III are calculated according to the method of Tusman et al. [49]. This method uses the third derivative of the volumetric capnogram and is schematically shown in figure 3.1. In this figure the starting point of phase II is defined as point B1 (the peak left to the negative peak of the third derivative). The starting point of phase III is defined as point B2 (the peak right to the negative peak of the third derivative). When the starting points of phase II and III are known, linear approximations of the phases are calculated. The slope of the linear approximation of phase II is set to the slope of the volumetric capnogram at the deflection point of the first derivative (point A in figure 3.1). To prevent that the linear approximation of phase III is influenced by the transition of phase II to III and small artefacts at the end of exhalations, the linear approximation of phase III was determined from the middle third portion of phase III using linear regression.

After determination of the linear approximations of phase II and III, Vd_{aw} is calculated using the method of Fletcher et al. [51]. The area between the linear approximation of phase III, the right of a virtual vertical line and the volumetric capnogram (area q in figure 2.5) and the area between the volumetric capnogram, the linear approximation of phase I and the right of the virtual vertical line (area p in figure 2.5) were calculated for several volumes. Afterwards, Vd_{aw} was set to the volume at which the absolute difference in areas was minimal.

From all parameters the average values of all 10 exhalations were used for statistical analysis.

3.2.3 New Parameter

In a interim analysis, body weight seemed to be unequal distributed between the no PE and the PE groups. As weight highly influences several respiratory physiologic processes [52], a combination of parameters which theoretically should diminish this effect was sought-after. After analysis of the theoretic influence of body weight and lowered perfusion on the several volumetric capnography parameters, a combination of respiratory rate, amount of CO_2 exhaled per breath, and the slope of phase III was made. The influence of both increase in weight and lowered pulmonary perfusion is provided in table 3.1. An increase in body weight is not known to influence RR in a substantial manner. A lowered perfusion however, in the case of PE, will cause hyperventilation as less CO_2 can be exhaled per breath when a normal minute volume is maintained. In the case of PE, thoracic

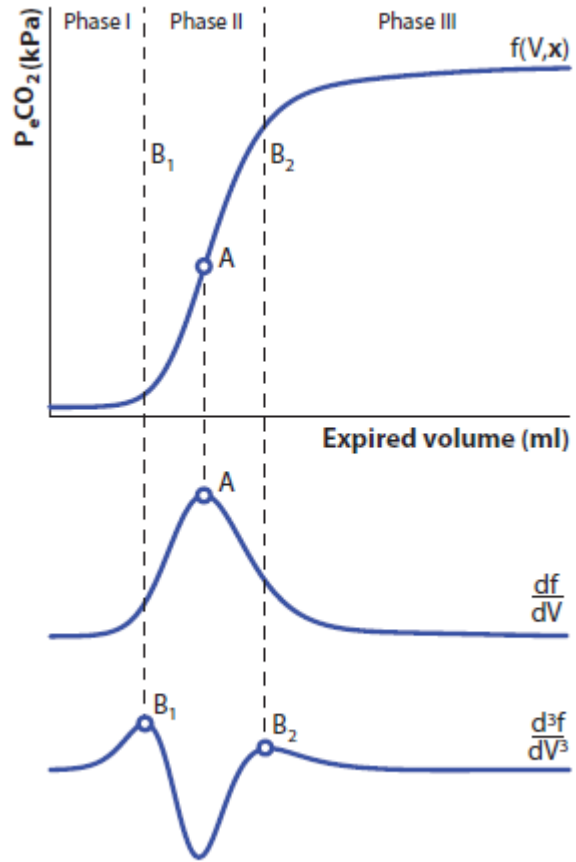


Figure 3.1: Determination of the starting points of phase II and III following the method of Tusman et al. [49]. The starting point of phase II is defined as point B1 (the peak left to the negative peak of the third derivative). The starting point of phase III is defined as point B2 (the peak right to the negative peak of the third derivative). Copied from BJM Hermans [50].

Table 3.1: Influence of increase in body weight and decrease of pulmonary perfusion on the respiratory rate (RR), amount of CO_2 exhaled per breath (V_{CO_2}) and the slope of phase III (slope III).

	Weight ↑	Perfusion ↓
RR (breaths/min)	↓ / = / ↑	↑
V_{CO_2} (mL/breath)	↑	↓
Slope III (kPa/L)	↓	↓

pain is often present making an increase in RR more likely than an increase in tidal volume. As the amount of CO_2 produced by the body per minute (which should be equal to the amount of exhaled CO_2 per minute) does not change, the amount of CO_2 exhaled per breath decreases. The production of CO_2 is known to be dependent on body weight, i.e. a high body weight indicates a high amount of CO_2 exhaled per minute (and thus per breath as RR is not influenced per se). An increase in weight also limits pulmonary perfusion and therefore the effect of PE and increase in weight are identical for the slope of phase III of the volumetric capnogram (which is a measure for pulmonary perfusion [53]) [54].

With the theoretic influence of weight and PE on these parameters a combination theoretically independent to weight and highly dependent to PE was made (as depicted in equation 3.3).

$$\text{New Parameter} = \frac{V_{CO_2} \times \text{slopeIII}}{RR} \quad (3.3)$$

An increase in weight should not influence the new parameter as V_{CO_2} increases and slope III decreases. The presence of PE should result in a decrease in the new parameter as both V_{CO_2} and slope III decrease and RR increases.

3.3 Statistical Analysis

Data were tested for normal distribution by visual inspection of histograms. If normally distributed, independent-samples t-tests was performed on the continuous variables to test if the mean of the parameters differ between the PE and no PE groups. If not normally distributed, distributions of the continuous variables in the no PE and PE groups were compared using the Mann-Whitney test. For the discrete variables a Fisher-exact test was performed. Correlation between the new parameter and the parameters of which it exists and body weight were tested using the Pearson correlation. Receiver operator characteristic curves were made for PET_{CO_2} and the $T_{L,NO}/T_{L,CO}$ ratio and all other parameters with statistically significant different distributions. Diagnostic values (sensitivity, specificity, negative predictive value and positive predictive value) of the several PET_{CO_2} thresholds and other significant parameters were calculated. P-values smaller than 0.05 were considered statistically significant. All statistic analyses were performed using SPSS Statistics 22⁴.

⁴SPSS Inc, Chicago, Illinois, USA

Chapter 4

Results

Patients were included from the begin of August 2014 till the end of April 2015. During this period, 36 patients were approached for participation in this study. Five of the approached patients refused participation leading to 31 included patients in which 13 PE was seen on CTPA. The characteristics of the included patients are provided in table 4.1.

Table 4.1: Patient characteristics. Data are presented as median (interquartile range) unless stated otherwise. Means and standard deviations of the continuous variables in the no PE and PE groups are compared using independent-samples t-tests. Distributions of sex and currently smoking in the no PE and PE groups are compared using chi-square tests. * indicates a statistically significant difference ($p < 0.05$). BMI denotes the body mass index.

	<i>No PE (N=18)</i>		<i>PE (N=13)</i>		<i>p-value</i>
Age (y)	56	(43 - 71)	50	(41 - 69)	0.508
Females (N (%))	10	(55.6)	6	(46.2)	0.605
Height (cm)	176	(166 - 183)	177	(167 - 183)	0.602
Weight (kg)	82	(73 - 94)	76	(64 - 96)	0.280
BMI (kg/m ²)	28.6	(24.2 - 32.6)	25.2	(22.1 - 28.0)	0.072
Smoked last 12 hours (N (%))	6	(33.3)	2	(15,4)	0.412
Wells-score	3.0	(0.0 - 3.0)	3.0	(3.0 - 5.0)	0.011*
D-dimer ($\mu\text{g/L}$)	862	(647 - 1759)	3649	(1408 - 5918)	0.001*

4.1 CO/NO diffusion

CO/NO diffusion measurements failed in three patients (two no PE, one PE) due to technological difficulties. The results of the measurements are provided in table 4.2.

4.2 Volumetric capnography

A graphical user interface (GUI) was made in Matlab to simplify the analysis of the capnogram in Matlab. A screenshot of the GUI is provided in figure 4.1. The green background color indicates the measurements meet the validity criteria. If the data is found invalid, the background color becomes red and the parameter values are not displayed, making the use of inappropriate data impossible.

The results of the volumetric capnography measurements are provided in table 4.3. Analysis of phase III of the capnogram was not possible in one patient due to a very high respiratory rate. The Pearson correlation between weight and the parameters which are combined in the new parameter

is provided in table 4.3. As PE also influences the value of these parameters, the Pearson correlation is separately calculated for the PE and no PE groups. Weight was significantly correlated with VCO_2 in both the no PE and the PE group. The slope of phase III was borderline significantly correlated with weight in the PE group. The receiver operating characteristic curve of PET_{CO_2} and the new parameter are provided in figure 4.2. Area under the curve (AUC) of PET_{CO_2} was 0.69 (95% confidence interval (CI) 0.50 - 0.88) and was not statistically significant higher than 0.50 ($p=0.075$). AUC of the new parameter was 0.79 (95% CI 0.64 - 0.95) and was statistically significant higher than 0.50 ($p=0.006$). A cut-off value of the new parameter to exclude PE was chosen as the lowest value with 100% sensitivity (i.e. all PE subjects had a value of the new parameter below this value). This threshold was 1.9 kPa.s/L which results in a sensitivity of 100%, a specificity of 47%, a positive predictive value (PPV) of 54% and a negative predictive value (NPV) of 100%. The diagnostic values (sensitivity, specificity, PPV and NPV) of PET_{CO_2} higher than thresholds reported in literature are provided in table 4.5. The exact test results (true positive, false positive, true negative, false negative) of the only PET_{CO_2} threshold without false negatives and the new parameter using a cut-off value of 1.9 kPa.s/L to exclude PE are provided in 2x2 tables in table 4.6.

Table 4.2: Results of the CO/NO diffusion measurements. Data are presented as median (interquartile range) unless stated otherwise. Distributions of the continuous variables in the no PE and PE groups are compared using the Mann-Whitney test. * indicates a statistically significant difference ($p < 0.05$). VA denotes the alveolar volume, %R the percentage of a value compared to its predicted value, $T_{L,CO}$ the transfer factor of the lungs for carbon monoxide, K_{CO} the transfer coefficient of the lungs for carbon monoxide, $T_{L,NO}$ the transfer factor of the lungs for nitric oxide and K_{NO} the transfer coefficient of the lungs for nitric oxide.

	<i>No PE (N=16)</i>		<i>PE (N=12)</i>		<i>p-value</i>
VA (L)	4.79	(3.96 - 5.19)	4.40	(3.53 - 5.57)	0.516
VA % R	77.1	(65.5 - 87.8)	71.0	(65.0 - 81.4)	0.353
$T_{L,CO}$ (mmol/kPa/min)	7.16	(5.27 - 8.90)	6.62	(5.21 - 7.45)	0.330
$T_{L,CO}$ % R	75.8	(62.9 - 89.6)	68.8	(58.5 - 75.7)	0.120
K_{CO} (mmol/kPa/min/L)	1.47	(1.35 - 1.62)	1.46	(1.20 - 1.80)	0.926
K_{CO} % R	99.9	(85.8 - 111.7)	100.5	(87.7 - 107.3)	0.610
$T_{L,NO}$ (mmol/kPa/min)	29.9	(23.0 - 37.9)	25.8	(20.0 - 30.3)	0.286
$T_{L,NO}$ % R	69.3	(57.0 - 76.1)	60.5	(46.6 - 68.9)	0.078
K_{NO} (mmol/kPa/min/L)	6.10	(5.24 - 7.10)	5.98	(5.33 - 6.81)	0.642
K_{NO} % R	89.5	(76.4 - 95.5)	83.9	(77.0 - 91.1)	0.330
$T_{L,NO}/T_{L,CO}$	4.09	(3.83 - 4.40)	4.00	(3.78 - 4.32)	0.959

Table 4.3: Results of the volumetric capnography measurements. Data are presented as median (interquartile range) unless stated otherwise. Distributions of the continuous variables in the no PE and PE groups are compared using the Mann-Whitney test. * indicates a statistically significant difference ($p < 0.05$). RR denotes the respiratory rate, V_T the tidal volume per kilogram weight, VD_{aw} the calculated anatomical dead space, PET_{CO_2} the end-tidal partial CO_2 pressure in expired air, Slope III the slope of the linear approximation of phase III of the volumetric capnogram and VCO_2 the amount of expired CO_2 per breath.

	<i>No PE (N=18)</i>		<i>PE (N=13)</i>		<i>p</i> -value
RR (breaths/min)	15.1	(12.0 - 17.3)	17.1	(14.4 - 17.9)	0.123
VT (mL/kg)	7.84	(6.08 - 9.33)	7.89	(6.12 - 9.30)	0.889
PETCO ₂ (kPa)	4.37	(4.00 - 4.83)	4.07	(3.37 - 4.38)	0.075
VCO_2 (mL/breath)	16.6	(11.8 - 19.8)	12.2	(10.7 - 16.9)	0.155
VDaw (mL/kg)	2.68	(2.32 - 3.07)	2.98	(2.60 - 3.33)	0.149
VDaw/VT	0.33	(0.31 - 0.40)	0.39	(0.32 - 0.47)	0.269
Slope III (kPa/L)	1.30	(0.99 - 2.50)	1.70	(0.91 - 2.30)	0.950
VCO_2 * slopeIII / RR	1.85	(1.21 - 3.00)	1.18	(0.61 - 1.38)	0.006*

Table 4.4: Pearson correlation of RR, VCO_2 , slope III and their combination in the new parameter with weight. Data are presented as the Pearson correlation of the variable with weight (p-value). Correlations with p-values < 0.05 are considered statistically significant and denoted with *.

	<i>No PE (N=18)</i>		<i>PE (N=13)</i>	
RR	-0.042	(0.872)	-0.427	(0.145)
VCO_2	0.514	(0.035)*	0.572	(0.041)*
Slope III	-0.082	(0.755)	-0.542	(0.055)
$\frac{VCO_2 \times \text{slopeIII}}{RR}$	0.292	(0.256)	0.065	(0.833)

Table 4.5: Diagnostic values of the thresholds for PET_{CO_2} as suggested by Rumpf et al., Hemnes et al. and Riaz and Jacob and the new parameter to exclude PE in our data (no PE N=17, PE N=13). Sens denotes sensitivity, Spec specificity, PPV positive predictive value and NPV negative predictive value.

<i>Author</i>	<i>Threshold</i>	<i>Sens</i>	<i>Spec</i>	<i>PPV</i>	<i>NPV</i>
Rumpf et al. [43]	>3.7 kPa	38%	82%	63%	64%
Hemnes et al. [44]	≥ 4.8 kPa	100%	24%	50%	100%
Riaz and Jacob [45]	>4.3 kPa	62%	53%	50%	64%
New Parameter	>1.90	100%	47%	54%	100%

Table 4.6: Diagnostic values of the PET_{CO_2} threshold as suggested in literature and the new established parameter.

(a) 2x2 table using the cut-off value of the $PET_{CO_2} \geq 4,8$ kPa to exclude pulmonary embolism as proposed by Hemnes et al [44]. This cut-off value yields a sensitivity of 100%, a specificity of 24%, a negative predictive value of 100% and a positive predictive value of 50%.

	<i>PE</i>	<i>no PE</i>
$PET_{CO_2} < 4.8$	13	13
$PET_{CO_2} \geq 4.8$	0	4

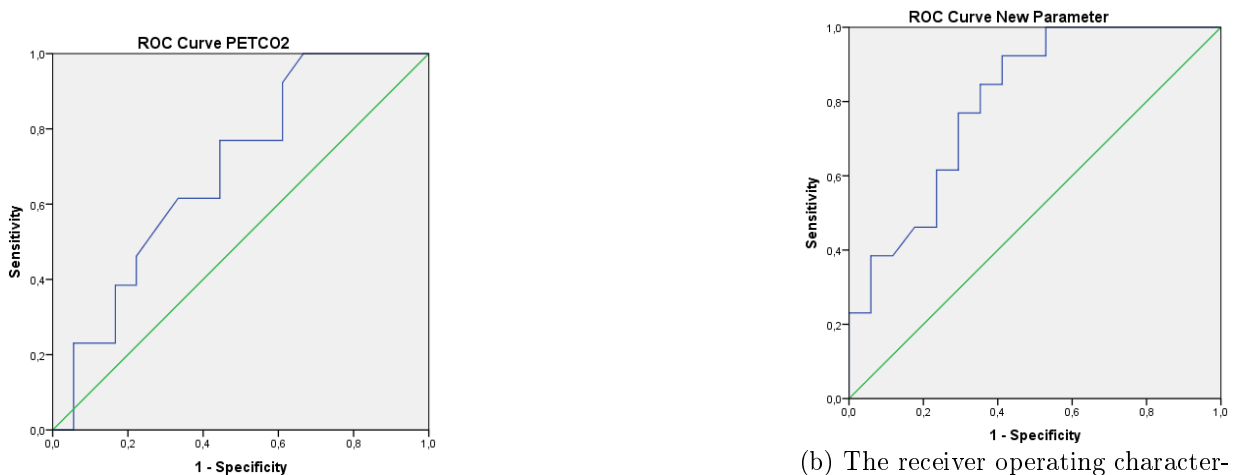
(b) 2x2 table using a cut-off value of the new parameter $\frac{VCO_2 \times \text{slopeIII}}{RR} > 1.9$ kPa.s/L to exclude pulmonary embolism. This cut-off value yields a sensitivity of 100%, a specificity of 47%, a negative predictive value of 100% and a positive predictive value of 54%.

	<i>PE</i>	<i>no PE</i>
$\frac{VCO_2 \times \text{slopeIII}}{RR} \leq 1.9$	13	9
$\frac{VCO_2 \times \text{slopeIII}}{RR} > 1.9$	0	8



Figure 4.1: A screenshot of the graphical user interface in Matlab which was used to analyse the volumetric capnography data.

Figure 4.2: ROC curves of PET_{CO_2} and the new parameter.



(a) The receiver operating characteristic (ROC) curve of PET_{CO_2} . Area under the curve (AUC) is 0.69 (95% CI 0.50 - 0.88, $p = 0.075$)

(b) The receiver operating characteristic (ROC) curve of the new parameter $\frac{V_{CO_2} \times slope_{III}}{RR}$. Area under the curve (AUC) is 0.79 (95% CI 0.64 - 0.95, $p = 0.006$)

Chapter 5

Discussion

5.1 Patient Characteristics

In table 4.1 it can be seen that age, sex, height and weight (though an interim analysis showed different distributions) are equally distributed between the PE and no PE groups. The number of patients who smoked in the last 12 hours is due to the low number of smokers not significantly different but twice as high in the no PE group compared to the PE group. The body mass index (BMI) is borderline significant ($p=0.072$) lower in the PE group compared to the no PE group. Nevertheless, the difference in BMI is relatively small and indicates a healthy average BMI in the PE group and mild overweight in the no PE group. As an increased BMI is associated with a lowered physical status, this might explain the high BMI in the no PE group, which essentially is a group of subjects without PE but with complaints/symptoms. As expected, both Wells-score and D-dimer are significantly higher in the PE group compared to the no PE group. It has to be noted that (due to the inclusion criteria of the study) all but one patient (this patient had a Wells-score of 10.5 making D-dimer evaluation superfluous) had increased D-dimer ($\geq 500 \mu\text{g/L}$). Use of the age-adjusted D-dimer cut-off (if aged > 50 , D-dimer is elevated if $> \text{age in years} \times 10$) would have ruled out PE in one patient of the no PE group.

5.2 CO/NO diffusion

Due to the results of Harris et al. and the physiological theory behind the $T_{L,NO}/T_{L,CO}$ ratio, it was expected that the ratio is increased in PE compared to no PE patients. Our data show lowered $T_{L,CO}$ and $T_{L,NO}$, and normal $T_{L,NO}/T_{L,CO}$ ratios in both groups (as can be seen in table 4.2).

The value of $T_{L,CO}$ in PE has been investigated several times. Wimalaratna et al. for instance reported a $T_{L,CO}$ of less than 75% of predicted in PE patients which failed to normalize to normal values within three months in most cases [55]. Oppenheimer et al. report decreased $T_{L,CO}$ values in chronic thromboembolic disease [56] but it is hard to compare these values to acute PE. In 2011, Piirilä et al. reported lowered $T_{L,CO}$ in acute PE similar to the values found by Wimalaratna et al. (74% of predicted) which were still lowered after seven months [57]. The $T_{L,CO}$ values we found (69% of predicted) are comparable with the results of both Wimalaratna et al. and Piirilä et al. In the publication of Piirilä et al., all values (including Dm and Vc) are also reported for a healthy control group. They did not find a significant difference in Dm/Vc ratio (to which the $T_{L,NO}/T_{L,CO}$ ratio is dependent) and Vc between the PE group and the healthy controls. Nevertheless, they did find significant lower values of Dm between the PE group and healthy controls in both the acute phase and after seven months. Moreover, they report a (weak) correlation between Dm and the extent of the pulmonary embolism measured by central embolism mass ($r=0.31$, $p=0.047$).

Piirilä et al. argue that Dm is influenced more by the reduction in alveolar volume compared to Vc . As $T_{L,NO}$ is directly related to Dm , this argument agrees with the finding of Hughes et al. that $T_{L,NO}$ is influenced more by reduction in alveolar volume than $T_{L,CO}$ [48]. Concluding, the present findings do not correspond with the data of Harris et al. found in sheep but are consistent with earlier measurements of $T_{L,CO}$ in pulmonary embolism in humans.

First of all, a probable cause of the lack in increased $T_{L,NO}/T_{L,CO}$ ratios might be the relatively

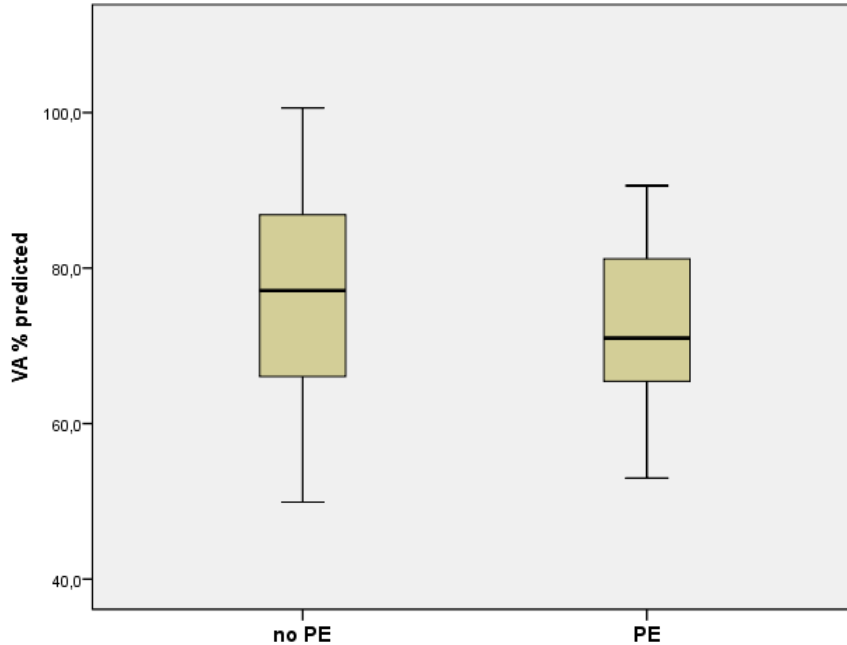


Figure 5.1: Boxplots of the distribution of the measured alveolar volume relative to its predicted value.

low severity of the pulmonary emboli included in this study, as hemodynamic unstable and oxygen dependent patients were excluded. Moreover, recent research showed that only total occluding emboli result in perfusion defects [58] making changes in gas exchange unlikely in non-occluding emboli. Finally, hypocapnic bronchoconstriction might shift ventilation towards well perfused regions [59] which could also diminish the negative effects of PE on the diffusion capacity of the lungs.

Detailed inspection of the now presented data reveal another possible explanation for the lack in increased $T_{L,NO}/T_{L,CO}$ ratios. The measured alveolar volume is decreased in both groups (77.1 % of predicted in the no PE group vs 71.0 % of predicted in the PE). An overview of the distribution of the alveolar volume in both groups is provided in figure 5.1. This decreased alveolar expansion is likely to be caused by the thoracic pain of which almost all patients suffered. A reduced alveolar volume greatly influences the measured transfer factors. A reduction of alveolar volume will decrease the surface area and increase the thickness of the alveolar-capillary membrane (and therefore decreases Dm and thus $T_{L,NO}$). $T_{L,CO}$ is approximately equal dependent on Dm and Vc and is therefore less dependent on a decrease in alveolar volume. Thus, the $T_{L,NO}/T_{L,CO}$ ratio decreases with a decrease in alveolar volume. [48,60] This might explain the slightly lowered $T_{L,NO}/T_{L,CO}$ ratios found in our data. In the data of van der Lee et al. an alveolar volume of 70-80 % of its value at total lung capacity (TLC) results in a measured $T_{L,NO}/T_{L,CO}$ ratio of approximately 4.00 [48] which corresponds with the now presented data. The previous reports of Wimalaratna and Piirilä et al. on $T_{L,CO}$ in PE do not report alveolar volumes compared to

its predicted value. However, in both publications, the measured alveolar volume compared to its predicted value is not reported. They do report K_{CO} and its predicted value. Piirilä et al. report normal K_{CO} values indicating decreased alveolar volume which corresponds with our data. Surprisingly, Wimalaratna et al. report lowered K_{CO} values when compared to their predicted value (calculated from mean data). This difference can be caused by changes between 1989 and now in measurement protocol and the reference equations used to calculate predicted values.

The transfer coefficient K (T_L divided by alveolar volume), is often used to discriminate between loss of volume (decreased T_L but normal K) and loss of function (both T_L and K decreased). Given that K_{CO} is normal in both the no PE and the PE group, it seems that it may be concluded that the decrease in $T_{L,CO}$ (and even higher decrease in $T_{L,NO}$) is caused by loss of volume. However, dividing T_L by alveolar volume does not eliminate the influence of alveolar volume on the outcome [61,62]. A (voluntary) decreased expansion will result in a linear decrease of T_L and an exponential increase of K . [63] Van der Lee et al. have made equations to calculate $T_{L,CO}$ and $T_{L,NO}$ at TLC when a measured $T_{L,CO}$, $T_{L,NO}$ and VA relative to its value at TLC are known [48]. Using these equations on the now presented data yields a median corrected $T_{L,CO}$ of 90.5% of predicted (IQR 78.9 - 99.9) in the no PE group versus 82.9% of predicted (IQR 77.6 - 87.5) in the PE group ($p=0.086$), a median corrected $T_{L,NO}$ of 83.8% of predicted (IQR 74.8 - 91.0) in the no PE group versus 79.1% of predicted (IQR 74.0 - 85.6) in the PE group ($p=0.227$) and a median corrected $T_{L,NO}/T_{L,CO}$ ratio of 4.51 (IQR 4.05 - 4.80) in the no PE group versus 4.43 (IQR 4.26 - 4.79) in the PE group ($p=1.000$). It can be seen that, even with the correction for decreased alveolar volume, no differences in $T_{L,NO}/T_{L,CO}$ ratio was found. Moreover, differences in $T_{L,NO}$ compared to its predicted values between the PE and no PE groups are smaller with higher p-value. $T_{L,CO}$ compared to predicted however becomes border-line significantly lower in the no PE group (which is consistent with the earlier mentioned studies on $T_{L,CO}$ in PE). Summarizing, the corrected data indicate that the borderline significant difference in $T_{L,NO}$ between the PE and no PE group is caused by the decrease in alveolar volume. Nevertheless, the corrected $T_{L,NO}/T_{L,CO}$ ratio shows no differences between the PE and no PE group. However, these equations are not externally validated. Moreover, the value of VA at TLC is needed and it is questionable whether the predicted value of VA can be used as a substitute. Therefore, it is hard to draw any conclusions from the corrected data.

A remark on the single-breath CO/NO-diffusion measurement procedure needs to be made. A breath hold time of 10 seconds was used whereas the fast decay of NO might warrant shorter breath hold times. Dressel et al. found higher $T_{L,NO}$ values when a breath hold time of four seconds was used compared to a breath hold time of 10 seconds, and no difference in $T_{L,NO}$ between six or eight seconds breath hold [64]. These findings have not been reproduced since. Therefore, Hughes and van der Lee recommended the use of 10 seconds breath hold to enable comparison with $T_{L,CO}$ values found in previous research [8]. Nevertheless, due to its fast decay, the amount of NO might fall below detectable limits. The manual of the MasterScreenTM PFT Pro system reports a lower limit of detection for NO of 0.0 ppm. However, its software marks fractions lower than 1.0 ppm as unreliable. Analysis of the now presented data shows a median expired NO fraction of 1.73 (IQR 1.25 - 2.22) ppm which is above the lower detection limit of the NO sensor of the MasterScreenTM PFT Pro system. Nevertheless, this is the median value of NO in the sample volume. Though the decay of NO is exponential and is therefore not likely to be significantly decreased at the end of the sample volume compared to the median of the sample volume, values at end sample volume are more interesting as they are the lowest measured value. An attempt to obtain these the lowest NO fractions was made by recording the raw signals. Unfortunately, these values could not be determined as the lowest values in the raw recordings were higher than the used values reported by the software. Apparently, a correction for an unknown measurement error is used by the software. Nevertheless, as the median measured NO fraction (which is used for calculations) is above the

lower detection limit, it seems unlikely that the breath hold time influenced the outcomes of this study.

5.3 Volumetric capnography

Based on earlier literature, it was expected that PET_{CO_2} was low in PE patients compared to the patients in which PE was excluded. Our data on PET_{CO_2} do not show this difference (table 4.3). Though no statistical significant difference in any of the volumetric capnography parameters between the subjects with proven PE and the subjects without proven PE was found, our novel parameter $\frac{V_{CO_2} \times slope_{III}}{RR}$ shows promising results. The ROC of this parameter is provided in figure 4.2b. As PE is a potentially lethal pathology, a threshold providing a negative predictive value (NPV) of 100% is warranted. The lowest threshold providing this was a value of 1.90 kPa.s/L or higher to exclude PE, resulting in eight true negative subjects (44% of all no-PE subjects). This seems to indicate that using this parameter might substantially decrease the need for CTPA to exclude PE.

The value of PET_{CO_2} alone to exclude PE seems limited. Both the threshold of Riaz et al. of PET_{CO_2} higher than 4.3 kPa [45] and the suggested cut-off of Rumpf et al. of PET_{CO_2} higher than 3.7 kPa and low clinical probability [43] to exclude PE, result in five (38%) false-negative subjects. Our data is more consistent with the threshold of Hemnes et al. who proposed that a threshold of PET_{CO_2} higher than 4.8 kPa might safely rule out pulmonary embolism [44]. Our data support this claim but it has to be noted that only four no PE patients (24%) had a PET_{CO_2} above 4.8 kPa. Using this threshold will therefore not result in any added clinical value (according to our data). The differences in results might be caused by the time of measurement. In our study volumetric capnography was always performed in the acute phase (either within 2 hours of the filing of the CTPA request when prehydration was warranted or otherwise directly after the CTPA) whereas several other studies performed the measurements within 24 hours of the CTPA. The symptoms of the non-PE subjects might have normalized during the 24 hours between the CTPA and the measurement. From our data it can be concluded that almost all patients with clinical suspicion of PE (supported by either an elevated D-dimer or Wells-score) had a lowered PET_{CO_2} . Given that most of these patients are dyspnoeic (often one of the reasons of their presence at the emergency department), this finding seems plausible. We question therefore the usability of PET_{CO_2} to discriminate between PE and non-PE patients in the acute phase. However, the difference might also be caused by the fact that other studies are performed by emergency department staff, including all patients with suspicion on PE. In our study only patients with suspicion on PE seen by a pulmonologist were included. One might reason that patients initially seen by a cardiologist or internist have lower probability of being dyspnoeic (and therefore have a lower probability for having a lowered PET_{CO_2}) than patients seen by a pulmonologist.

Another cause may be the extent of the emboli. Due to the exclusion criteria used in this study, it is likely that only low and moderate risk PE was included. Using dual energy CTPA, Ikeda et al. have shown that in non-occluding emboli, pulmonary blood flow is preserved [58]. Even if total-occluding emboli are present, ventilation may shift to better perfused regions due to hypocapnic bronchoconstriction [59]. Both mechanisms will reduce the effect of the emboli on respiratory physiology and may therefore result in only little abnormalities of the volumetric capnogram.

Despite these possible compensatory mechanisms and low extent of the emboli, our novel parameter $\frac{V_{CO_2} \times slope_{III}}{RR}$ showed promising results. This parameter was designed to remove the possible biasing influence of weight on the outcome of the volumetric capnography. As can be seen in table 4.4, weight only significantly correlates with V_{CO_2} in both the no PE and PE group. This correlation is positive, which corresponds with the theory that the amount of CO_2 exhaled per breath increases with body weight. The slope of the linear approximation of phase III has a

significant negative correlation with weight in the PE group. The negative correlation was expected but also for the no PE group. That this correlation is not found in the no PE group might be caused by the higher percentage of smokers in the no PE group (though not statistically significant). As expected, respiratory rate does not correlate significantly with body weight in both the PE and no PE group. The new parameter also does not correlate with weight, which was the aim of its design. It seems therefore safe to conclude that weight has no (or at the most little) influence on the difference in the significant lower values of the new parameter in the PE group. Some threshold for the new parameter had to be determined to be able to safely exclude PE when the new parameter lies above this value. This value was found to be 1.90 kPa.s/L, providing a sensitivity of 100% and specificity of 47% (see tables 4.5 and 4.6). This means that no patients with a new parameter above 1.90 kPa.s/L had PE and 47% of all patients with PE had a new parameter above 1.90 kPa.s/L. If no CTPA would have been made when the new parameter was above the established threshold, CTPA would have shown PE in 59% of the subjects which is more than double of the maximal 25% positives which are seen nowadays. Summarizing, the use of the new parameter could have prevented 47% of the CTPA in the no PE group which is a significant reduction.

One can argue that CTPA might also reveal other pathology explaining the symptoms. Van Es et al. have shown that such findings are found in almost one-half of all CTPAs requested due to suspected PE. However, these findings had therapeutic consequences in less than 1% of the patients. [65] Recent research focusing on the decrease in CTPA has suggested an age-adjusted D-Dimer cutoff [14] which has not yet been adopted in our hospital. Nevertheless, using it would not have resulted in a decrease in CTPA as all D-Dimer were higher than the age-adjusted cutoff. Therefore it seems safe to suggest that even with the age-adjusted D-Dimer cutoff, our parameter might have added value. Nevertheless, further investigation including the validation of the threshold in larger patient numbers is needed to confirm its applicability in the clinic.

Chapter 6

Conclusion

This study tried to answer the question whether CO/NO diffusion and volumetric capnography can safely exclude pulmonary embolism (PE) in patients at the emergency department to lower the number of expensive and potential harmful CTPA scans. For CO/NO diffusion the answer is no, it cannot be used to exclude PE. No difference in $T_{L,NO}/T_{L,CO}$ ratio was found. The lack in difference is likely to be caused by a decreased inspired volume due to the thoracic pain of which patients with suspicion on PE often suffer. The most often used parameter of volumetric capnography, PET_{CO_2} , has little added value according to our data. A new derived parameter, $\frac{V_{CO_2} \times slope_{III}}{RR}$, shows more promising results. Using a cut-off value of higher than 1.90 kPa.s/L to exclude PE results in a sensitivity of 100 % and a specificity of 47%. This indicates that in almost half of all subjects without PE, the new parameter could have safely excluded PE. However, as the threshold is retrospectively determined and the number of included subjects is small, prospective validation in a large sample size is needed to confirm its true usability.

Chapter 7

Future Research and Recommendations

The presented data allow to draw some conclusions but many aspects remain uncertain. Therefore, more research has to be performed.

A goal of this research project was to develop a method which enables the analysis of the exhaled NO fraction over a complete exhalation (instead of just a sample volume). This should enable to calculate $T_{L,NO}$ as a function of the exhaled volume. Due to technical difficulties, it was not possible to create the setup in during this internship. Nevertheless, equipment to enable this measurement exists and can be incorporated relatively easy in the current CO/NO-diffusion setup. As in PE not the entire pulmonary vasculature is obstructed by the emboli, it is expected that the $T_{L,NO}$ differs between the affected and unaffected lung regions. One could hypothesize that this can be seen in a plot of $T_{L,NO}$ (or perhaps the $T_{L,NO}/T_{L,CO}$ ratio) as a function of the exhaled volume, although mixing of healthy and affected lung regions will still occur (but on a smaller scale). If a setup to allow the calculation of $T_{L,NO}$ as a function of the exhaled volume is created, the influence of breath hold time on this curve should be investigated. As already described in chapter 5, the debate on which breath hold time should be used in the CO/NO diffusion manoeuvre is still ongoing. Again, the curve of $T_{L,NO}$ as a function of the exhaled volume could add more information to this discussion.

A strong recommendation which can be implemented immediately is to incorporate a correction for the dependence of both $T_{L,CO}$ and K_{CO} on reduced alveolar volumes (this can be done by using the formulas developed by Stam et al. [61] or van der Lee et al. [48]). In current practice, K_{CO} is used as a form of $T_{L,CO}$ independent on alveolar volume. However, as described in chapter 5, $T_{L,CO}$ linear declines with a decrease of alveolar volume whereas K_{CO} increases exponentially. A decreased $T_{L,CO}$ with a low normal K_{CO} which is now interpreted as a loss of diffusing capacity due to loss of volume is in reality also a sign of loss of function. If the decrease in $T_{L,CO}$ was really completely due to loss of volume, K_{CO} should be significantly increased (the increase in K_{CO} should even be higher than the decrease in $T_{L,CO}$).

In the case of the volumetric capnography, obviously the most important recommendation is that the developed new parameter has to be validated. A realistic first step could be the use of earlier volumetric capnography data in PE patients to perform retrospective validation. If this validation still shows promising results, a prospective study should be performed to confirm it. Though our results indicate that PET_{CO_2} cannot be used to exclude PE in normally breathing patients, it seems attracting to study PET_{CO_2} after some breath manoeuvres. For instance, one would expect that PET_{CO_2} after breath holding is lower in patients with PE compared to the patients without PE. Unfortunately, research has shown that the time one can hold their breath is not completely dependent to Pa_{CO_2} [66]. Therefore, PET_{CO_2} at end of breath hold is still variable in healthy subjects probably making it hard to draw conclusions from a low PET_{CO_2} at the end of breath hold. A fixed breath hold time (i.e. 10 seconds) might provide more reproducible results.

The last recommendations concern general recommendations on PE diagnosis and management. First of all, age-adjusted D-dimer cutoffs should be implemented to lower the number of negative CTPA. Though research has shown the safety of such age-adjusted threshold, debate still exists if the threshold can be used in all D-dimer analysis methods. For the local policy, this could be relatively easy solved by analyzing all the D-dimer values of the past year where CTPA was also made. If similar results to the earlier mentioned research are obtained, the threshold should be implemented as soon as possible. Finally, as stated in chapter 5, the severity of the emboli included in this study was relatively low (i.e. only patients with moderate or low risk on adverse outcome were included). The now existing risk stratification is based on global parameters such as clinical scores (e.g. the PESI score) and signs of failure of the right ventricle. In some cases, for instance in isolated subsegmental emboli it is not clear whether treatment is necessary. Nevertheless, with its potentially lethal outcome, very few medical doctors dare not to treat these cases. Another example is the decision when to use direct thrombolysis in intermediate high risk patients. Evidence on the benefits of thrombolysis is substantial (i.e. lowered mortality) but the evidence on increased bleeding risks and thus adverse outcome is also substantial. Currently, thrombolysis is advised only in hemodynamic unstable patients. However, the definition of hemodynamic stability is vague. A risk stratification incorporating more functional information could theoretically clarify both problems. A possible route to obtain this information is quantification of the decrease in flow (or affected area or increase in pressure in the pulmonary artery) caused by the pulmonary emboli.

Acknowledgments

I would like to thank all who have supported me during this internship. A special thanks goes to:

- F.H.C. de Jongh, PhD, for daily support and supervising the physiologic/technical part of this thesis;
- M.M.M. Eijsvogel, MD, for daily support and supervising the medical part of this thesis;
- M. Brusse-Keizer, PhD, for assistance in the statistical analysis;
- M. Groenier, PhD, for the guidance in the development of my professional behavior;
- I. van der Lee, MD, PhD, for supervising the analysis of the diffusion measurements;
- R. Yohanna, MD, for being my clinical buddy;
- M. Vlutters, for teaching how to perform CO/NO diffusion measurements and troubleshooting;
- M. Mulder and M. Eitink for assisting in the regulatory part of the study;
- The complete staff of the pulmonary department of the Medisch Spectrum Twente for providing patients for this thesis and giving me the opportunity to learn more on pulmonary medicine;
- T. Bronsveld, MD, for his clinical view on the work of technical medicine students, providing me the opportunity to develop clinical experience and his contribution to the atmosphere in the basement;
- And finally, all fellow Technical Medicine interns: G. Snel, R. Bruggink, J. Benistant, M. Schreuders, O. Mennes, L. Hashemi, X. Hoppenbrouwer, E. Huizing and R. van Leuteren for all the help and the pleasant time I had during this internship.

Bibliography

- [1] P. D. Stein, R. D. Hull, K. C. Patel, R. E. Olson, W. A. Ghali, R. Brant, R. K. Biel, V. Bharadia, and N. K. Kalra, "D -Dimer for the Exclusion of Acute Venous Thrombosis and Pulmonary Embolism," *Annals of internal medicine*, vol. 140, pp. 589–602, 2004.
- [2] P. S. Wells, D. R. Anderson, M. Rodger, J. S. Ginsberg, C. Kearon, M. Gent, A. G. Turpie, J. Bormanis, J. Weitz, M. Chamberlain, D. Bowie, D. Barnes, and J. Hirsh, "Derivation of a simple clinical model to categorize patients probability of pulmonary embolism: increasing the models utility with the SimpliRED D-dimer.," *Thrombosis and haemostasis*, vol. 83, pp. 416–20, Mar. 2000.
- [3] A. Torbicki, A. Perrier, S. Konstantinides, G. Agnelli, N. Galiè, P. Pruszczyk, F. Bengel, A. J. B. Brady, D. Ferreira, U. Janssens, W. Klepetko, E. Mayer, M. Remy-Jardin, and J.-P. Bassand, "Guidelines on the diagnosis and management of acute pulmonary embolism: the Task Force for the Diagnosis and Management of Acute Pulmonary Embolism of the European Society of Cardiology (ESC).," *European heart journal*, vol. 29, pp. 2276–315, Sept. 2008.
- [4] P. D. Stein, S. E. Fowler, L. R. Goodman, A. Gottschalk, C. A. Hales, R. D. Hull, K. V. Leeper, J. Popovich, D. A. Quinn, T. A. Sos, H. D. Sostman, V. F. Tapson, T. W. Wakefield, J. G. Weg, and P. K. Woodard, "Multidetector Computed Tomography for Acute Pulmonary Embolism," *The New England journal of medicine*, vol. 354, no. 22, pp. 2317–2327, 2006.
- [5] E. D. Robin, D. G. Julian, D. M. Travis, and C. H. Crump, "A physiological approach to the diagnosis of acute pulmonary embolism," *The New England journal of medicine*, vol. 260, pp. 586–591, 1959.
- [6] A. Manara, W. D'hoore, and F. Thys, "Capnography as a diagnostic tool for pulmonary embolism: a meta-analysis," *Annals of emergency medicine*, vol. 62, pp. 584–91, Dec. 2013.
- [7] I. van der Lee, P. Zanen, J. C. Grutters, R. J. Snijder, and J. M. M. van den Bosch, "Diffusing capacity for nitric oxide and carbon monoxide in patients with diffuse parenchymal lung disease and pulmonary arterial hypertension.," *Chest*, vol. 129, pp. 378–83, Feb. 2006.
- [8] J. M. B. Hughes and I. van der Lee, "The TL,NO/TL,CO ratio in pulmonary function test interpretation.," *The European respiratory journal*, vol. 41, pp. 453–61, Feb. 2013.
- [9] R. S. Harris, M. Hadian, D. R. Hess, Y. Chang, and J. G. Venegas, "Pulmonary Atery Occlusion Increases the Ratio of Diffusing Capacity for Nitric Oxide to Carbon Monoxide in Prone Sheep," *Chest*, vol. 126, no. 2, pp. 559–565, 2004.
- [10] K. L. Moore, A. F. Dalley, and A. M. R. Agur, "Vasculature of lungs and pleurae," in *Clinically Oriented Anatomy*, ch. 1 - Thorax, pp. 116–118, Baltimore: Lippincott Williams & Wilkins, 6th ed., 2010.

- [11] P. Kumar and M. Clark, "Pulmonary Embolism," in *Clinical Medicine*, ch. 13, pp. 784–786, Saunders Elsevier, seventh ed., 2009.
- [12] G. Agnelli and C. Becattini, "Acute Pulmonary Embolism," *The New England journal of medicine*, vol. 363, pp. 266–74, 2010.
- [13] S. V. Konstantinides and A. Torbicki, "Management of pulmonary embolism: recent evidence and the new European guidelines.," *The European respiratory journal*, vol. 44, pp. 1385–90, Dec. 2014.
- [14] M. Righini, J. Van Es, P. L. Den Exter, P.-M. Roy, F. Verschuren, A. Ghuyssen, O. T. Rutschmann, O. Sanchez, M. Jaffrelot, A. Trinh-Duc, C. Le Gall, F. Moustafa, A. Principe, A. A. Van Houten, M. Ten Wolde, R. A. Douma, G. Hazelaar, P. M. G. Erkens, K. W. Van Kralingen, M. J. J. H. Grootenboers, M. F. Durian, Y. W. Cheung, G. Meyer, H. Bounameaux, M. V. Huisman, P. W. Kamphuisen, and G. Le Gal, "Age-adjusted D-dimer cutoff levels to rule out pulmonary embolism: the ADJUST-PE study.," *JAMA*, vol. 311, pp. 1117–24, Mar. 2014.
- [15] D. Levin, J. B. Seo, D. G. Kiely, H. Hatabu, W. Gefter, E. J. R. van Beek, and M. L. Schiebler, "Triage for suspected acute Pulmonary Embolism: Think before opening Pandora's Box.," *European journal of radiology*, vol. 84, pp. 1202–1211, June 2015.
- [16] S. Konstantinides, A. Torbicki, G. Agnelli, N. Danchin, D. Fitzmaurice, N. Galie, J. S. R. Gibbs, M. Huisman, M. Humbert, N. Kucher, I. Lang, M. Lankeit, J. Lekakis, C. Maack, E. Mayer, N. Meneveau, A. Perrier, P. Pruszczyk, L. H. Rasmussen, T. H. Schindler, P. Svitil, A. V. Noordegraaf, J. L. Zamorano, M. Zompatori, S. Achenbach, H. Baumgartner, J. J. Bax, H. Bueno, V. Dean, C. Deaton, C. Erol, R. Fagard, R. Ferrari, D. Hasdai, A. Hoes, P. Kirchhof, J. Knuuti, P. Kolh, P. Lancellotti, A. Linhart, P. Nihoyannopoulos, M. F. Piepoli, P. Ponikowski, P. A. Sirnes, J. L. Tamargo, M. Tendera, W. Wijns, S. Windecker, D. Jimenez, W. Ageno, S. Agewall, R. Asteggiano, R. Bauersachs, C. Becattini, H. Bounameaux, H. R. Buller, C. H. Davos, G.-J. Geersing, M. S. G. Sanchez, J. Hendriks, M. Kilickap, V. Mareev, M. Monreal, J. Morais, B. A. Popescu, O. Sanchez, A. C. Spyropoulos, N. Skoro-Sajer, R. Najafov, S. Sudzhaeva, M. De Pauw, F. Barakovi, M. Tokmakova, B. Skoric, R. Rokyta, M. L. Hansen, M. Elmet, V.-P. Harjola, G. Meyer, A. Chukhrukidze, S. Rosenkranz, A. Androulakis, T. Forster, F. Fedele, T. Sooronbaev, A. Maca, E. Ereminiene, J. Micallef, A. Andreasen, M. Kurzyna, D. Ferreira, A. O. Petris, S. Dzemeshevich, M. Asanin, I. Imkova, M. Anguita, C. Christersson, N. Kostova, H. Baccar, L. E. Sade, A. Parkhomenko, and J. Pepke-Zaba, "2014 ESC Guidelines on the diagnosis and management of acute pulmonary embolism: The Task Force for the Diagnosis and Management of Acute Pulmonary Embolism of the European Society of Cardiology (ESC) * Endorsed by the European Respiratory Society (ERS)," *European heart journal*, pp. 3033–3080, Aug. 2014.
- [17] D. Aujesky, D. S. Obrosky, R. a. Stone, T. E. Auble, A. Perrier, J. Cornuz, P.-M. Roy, and M. J. Fine, "Derivation and validation of a prognostic model for pulmonary embolism.," *American journal of respiratory and critical care medicine*, vol. 172, pp. 1041–6, Oct. 2005.
- [18] W. Zondag, L. M. A. Vingerhoets, M. F. Durian, A. Dolsma, L. M. Faber, B. I. Hiddinga, H. M. A. Hofstee, A. D. M. Hoogerbrugge, M. M. C. Hovens, G. Labots, T. Vlasveld, M. J. M. de Vreede, L. J. M. Kroft, and M. V. Huisman, "Hestia criteria can safely select patients with pulmonary embolism for outpatient treatment irrespective of right ventricular function.," *Journal of thrombosis and haemostasis*, vol. 11, pp. 686–92, Apr. 2013.

- [19] W. Zondag, I. C. M. Mos, D. Creemers-Schild, A. D. M. Hoogerbrugge, O. M. Dekkers, J. Dolsma, M. Eijsvogel, L. M. Faber, H. M. A. Hofstee, M. M. C. Hovens, G. J. P. M. Jonkers, K. W. van Kralingen, M. J. H. A. Kruij, T. Vlasveld, M. J. M. de Vreede, and M. V. Huisman, "Outpatient treatment in patients with acute pulmonary embolism: the Hestia Study," *Journal of thrombosis and haemostasis*, vol. 9, pp. 1500–7, Aug. 2011.
- [20] M. Krogh, "The diffusion of gases through the lungs of man," *Journal of physiology*, vol. 49, pp. 271–96, 1915.
- [21] J. M. B. Hughes and C. D. R. Borland, "The centenary (2015) of the transfer factor for carbon monoxide (TLCO): Marie Krogh's legacy," *Thorax*, vol. 70, pp. 391–4, Apr. 2015.
- [22] F. J. W. Roughton and R. E. Forster, "Relative importance of diffusion and chemical reaction rates in determining rate of exchange of gases in the human lung, with special reference to true diffusing capacity of pulmonary membrane and volume of blood in the lung capillaries," *Journal of applied physiology*, vol. 11, no. 2, pp. 290–302, 1957.
- [23] H. Guenard, N. Varene, and P. Vaida, "Determination of lung capillary blood volume and membrane diffusing capacity in man by the measurements of NO and CO transfer," *Respiration physiology*, vol. 70, pp. 113–120, Jan. 1987.
- [24] N. Macintyre, R. O. Crapo, G. Viegi, D. C. Johnson, C. P. M. van der Grinten, V. Brusasco, F. Burgos, R. Casaburi, A. Coates, P. Enright, P. Gustafsson, J. Hankinson, R. Jensen, R. McKay, M. R. Miller, D. Navajas, O. F. Pedersen, R. Pellegrino, and J. Wanger, "Standardisation of the single-breath determination of carbon monoxide uptake in the lung," *The European respiratory journal*, vol. 26, pp. 720–35, Oct. 2005.
- [25] T. van der Mark, M. Demedts, L. M. Lacquet, and L. Billiet, "Transferfactor (diffusiecapaciteit) van de long," in *Longfunctieonderzoek* (M. Demedts and M. Decramer, eds.), pp. 137–148, Leuven - Apeldoorn: Garant, 1st ed., 1998.
- [26] I. van der Lee, H. A. Gietema, P. Zanen, R. J. van Klaveren, M. Prokop, J.-W. J. Lammers, and J. M. M. van den Bosch, "Nitric oxide diffusing capacity versus spirometry in the early diagnosis of emphysema in smokers," *Respiratory medicine*, vol. 103, pp. 1892–7, Dec. 2009.
- [27] F. Verschuren, G. Liistro, R. Coffeng, F. Thys, J. Roeseler, F. Zech, and M. Reynaert, "Volumetric capnography as a screening test for pulmonary embolism in the emergency department," *Chest*, vol. 125, pp. 841–50, Mar. 2004.
- [28] W. S. Fowler, "Lung function studies - II The respiratory dead space," *Am J Physiol*, vol. 154, pp. 405–416, 1948.
- [29] R. Fletcher, *The single breath test for carbon dioxide*. Lund, Sweden: Berlings, Arlöv, second ed., 1986.
- [30] C. Bohr, "Ueber die Lungenathmung," *Skandinavisches Archiv fur Physiologie*, vol. 2, pp. 236–268, 1891.
- [31] H. Enghoff, "Volumen inefficax. Bermerkungen zur Frage des schädlichen Raumes," *Upsala Läkaefören. Förhandl.*, vol. 44, pp. 191–218, 1938.
- [32] H. T. Robertson, "Dead space: the physiology of wasted ventilation," *The European respiratory journal*, pp. 1–13, Nov. 2014.

- [33] G. Tusman, F. S. Sipmann, J. B. Borges, G. Hedenstierna, and S. H. Bohm, "Validation of Bohr dead space measured by volumetric capnography," *Intensive care medicine*, vol. 37, pp. 870–4, May 2011.
- [34] R. H. Kallet, R. R. T. Faarc, B. M. D. Rrt, O. G. Rrt, and M. A. Matthay, "Accuracy of Physiologic Dead Space Measurements in Patients With Acute Respiratory Distress Syndrome Using Volumetric Capnography : Comparison With the Metabolic Monitor Method," *Respiratory care*, vol. 50, no. 4, pp. 462–467, 2005.
- [35] S. H. Böhm, S. Maisch, A. von Sandersleben, O. Thamm, I. Passoni, J. Martinez Arca, and G. Tusman, "The effects of lung recruitment on the Phase III slope of volumetric capnography in morbidly obese patients.," *Anesthesia and analgesia*, vol. 109, pp. 151–9, July 2009.
- [36] D. O. Nutter and R. A. Massumi, "The Arterial-Alveolar Carbon Dioxide Tension Gradient in Diagnosis of Pulmonary Embolus," *Chest*, vol. 50, no. 4, pp. 380–387, 1966.
- [37] C. Colp and M. Stein, "Re-emergence of an Orphan Test for Pulmonary Embolism," *Chest*, vol. 120, no. 1, pp. 5–6, 2001.
- [38] J. A. Kline, S. Meek, D. Boudrow, D. Warner, and S. Colucciello, "Use of the Alveolar Dead Space Fraction (Vd/Vt) and Plasma D-dimers to Exclude Acute Pulmonary Embolism in Ambulatory Patients," *Academic emergency medicine*, vol. 4, pp. 856–863, Sept. 1997.
- [39] J. A. Kline, E. G. Israel, E. A. Michelson, B. J. O. Neil, M. C. Plewa, and D. C. Portelli, "Diagnostic Accuracy of a Bedside D-dimer Assay and Alveolar Dead-Space Measurement for Rapid Exclusion of Pulmonary Embolism," *JAMA*, vol. 285, no. 6, pp. 761–768, 2001.
- [40] K. Hogg, D. Dawson, T. Tabor, B. Tabor, and K. Mackway-jones, "in the Investigation of Pulmonary Embolism in Outpatients With Pleuritic Chest Pain," *Chest*, vol. 128, pp. 2195–2202, 2005.
- [41] F. Verschuren, O. Sanchez, M. Righini, E. Heinonen, G. Le Gal, G. Meyer, A. Perrier, and F. Thys, "Volumetric or time-based capnography for excluding pulmonary embolism in outpatients?," *Journal of thrombosis and haemostasis*, vol. 8, pp. 60–7, Jan. 2010.
- [42] F. Verschuren, E. Heinonen, D. Clause, F. Zech, M. S. Reynaert, and G. Liistro, "Volumetric capnography: reliability and reproducibility in spontaneously breathing patients.," *Clinical physiology and functional imaging*, vol. 25, pp. 275–80, Sept. 2005.
- [43] T. H. Rumpf, M. Krizmaric, and S. Grmec, "Capnometry in suspected pulmonary embolism with positive D-dimer in the field.," *Critical care*, vol. 13, p. R196, Jan. 2009.
- [44] A. R. Hemnes, A. L. Newman, B. Rosenbaum, T. W. Barrett, C. Zhou, T. W. Rice, and J. H. Newman, "Bedside end-tidal CO₂ tension as a screening tool to exclude pulmonary embolism.," *The European respiratory journal*, vol. 35, pp. 735–41, Apr. 2010.
- [45] I. Riaz and B. Jacob, "Pulmonary embolism in Bradford UK: role of end-tidal CO₂ as a screening tool," *Clinical medicine*, vol. 14, no. 2, pp. 128–33, 2014.
- [46] M. L. Pernoll, J. Metcalfe, P. A. Kovach, R. Wachtel, and M. J. Dunham, "Ventilation during rest and exercise in pregnancy and postpartum," *Respiration physiology*, vol. 25, no. 3, pp. 295–310, 1975.

- [47] R. E. Kanner and R. O. Crapo, "The relationship between alveolar oxygen tension and the single-breath carbon monoxide diffusing capacity," *American review of respiratory disease*, vol. 133, no. 4, pp. 676–678, 1986.
- [48] I. van der Lee, P. Zanen, N. Stigter, J. M. van den Bosch, and J.-W. J. Lammers, "Diffusing capacity for nitric oxide: reference values and dependence on alveolar volume.," *Respiratory medicine*, vol. 101, pp. 1579–84, July 2007.
- [49] G. Tusman, E. Gogniat, S. H. Bohm, A. Scandurra, F. Suarez-Sipmann, A. Torroba, F. Casella, S. Giannasi, and E. S. Roman, "Reference values for volumetric capnography-derived non-invasive parameters in healthy individuals.," *Journal of clinical monitoring and computing*, vol. 27, pp. 281–8, June 2013.
- [50] B. J. M. Hermans, "Patient specific optimal PEEP determination using volumetric capnography," tech. rep., University of Twente, Enschede, 2014.
- [51] R. Fletcher, B. Jonson, G. Cumming, and J. Brew, "The concept of deadspace with special reference to the single breath test for carbon dioxide," *British journal of anaesthesia*, vol. 53, no. 1, pp. 77–88, 1981.
- [52] K. Parameswaran, D. C. Todd, and M. Soth, "Altered respiratory physiology in obesity," *Canadian respiratory journal*, vol. 13, no. 4, pp. 203–210, 2006.
- [53] G. Tusman, F. Suarez-Sipmann, G. Paez, J. Alvarez, and S. H. Bohm, "States of low pulmonary blood flow can be detected non-invasively at the bedside measuring alveolar dead space.," *Journal of clinical monitoring and computing*, vol. 26, pp. 183–90, June 2012.
- [54] B. Babik, Z. Csorba, D. Czövek, P. N. Mayr, G. Bogáts, and F. Peták, "Effects of respiratory mechanics on the capnogram phases: importance of dynamic compliance of the respiratory system.," *Critical care*, vol. 16, p. R177, Jan. 2012.
- [55] H. S. Wimalaratna, J. Farrell, and H. Y. Lee, "Measurement of diffusing capacity in pulmonary embolism.," *Respiratory medicine*, vol. 83, pp. 481–5, Nov. 1989.
- [56] B. W. Oppenheimer, K. I. Berger, N. P. Hadjiangelis, R. G. Norman, D. M. Rapoport, and R. M. Goldring, "Membrane diffusion in diseases of the pulmonary vasculature.," *Respiratory medicine*, vol. 100, pp. 1247–53, July 2006.
- [57] P. Piirilä, M. Laiho, P. Mustonen, M. Graner, A. Piilonen, M. Raade, S. Sarna, V.-P. Harjola, and A. Sovijärvi, "Reduction in membrane component of diffusing capacity is associated with the extent of acute pulmonary embolism.," *Clinical physiology and functional imaging*, vol. 31, pp. 196–202, May 2011.
- [58] Y. Ikeda, N. Yoshimura, Y. Hori, Y. Horii, H. Ishikawa, M. Yamazaki, Y. Noto, and H. Aoyama, "Analysis of decrease in lung perfusion blood volume with occlusive and non-occlusive pulmonary embolisms.," *European journal of radiology*, vol. 83, pp. 2260–7, Dec. 2014.
- [59] J. Y. C. Tsang, W. J. E. Lamm, and E. R. Swenson, "Regional CO₂ tension quantitatively mediates homeostatic redistribution of ventilation following acute pulmonary thromboembolism in pigs.," *Journal of applied physiology*, vol. 107, pp. 755–62, Sept. 2009.
- [60] S. N. Glénet, C. De Bisschop, F. Vargas, and H. J. P. Guénard, "Deciphering the nitric oxide to carbon monoxide lung transfer ratio: physiological implications.," *The journal of physiology*, vol. 582, pp. 767–75, July 2007.

- [61] H. Stam, V. Hrachovina, T. Stijnen, and A. Versprille, “Diffusing capacity dependent in normal subjects on lung volume and age,” *Journal of applied physiology*, vol. 76, pp. 2356–2363, 1994.
- [62] D. C. Johnson, “Importance of adjusting carbon monoxide diffusing capacity (DLCO) and carbon monoxide transfer coefficient (KCO) for alveolar volume,” *Respiratory medicine*, vol. 94, pp. 28–37, Jan. 2000.
- [63] J. M. B. Hughes and N. B. Pride, “Examination of the carbon monoxide diffusing capacity (DL(CO)) in relation to its KCO and VA components,” *American journal of respiratory and critical care medicine*, vol. 186, pp. 132–9, July 2012.
- [64] H. Dressel, L. Filser, R. Fischer, D. de la Motte, W. Steinhäusser, R. M. Huber, D. Nowak, and R. A. Jörres, “Lung diffusing capacity for nitric oxide and carbon monoxide: dependence on breath-hold time,” *Chest*, vol. 133, pp. 1149–54, May 2008.
- [65] J. van Es, R. A. Douma, S. M. Schreuder, S. Middeldorp, P. W. Kamphuisen, V. E. A. Gerdes, and L. F. M. Beenen, “Clinical impact of findings supporting an alternative diagnosis on CT pulmonary angiography in patients with suspected pulmonary embolism,” *Chest*, vol. 144, pp. 1893–9, Dec. 2013.
- [66] M. J. Parkes, “Breath-holding and its breakpoint,” *Experimental physiology*, vol. 91, pp. 1–15, Jan. 2006.
- [67] W. F. Boron and E. L. Boulpaep, “Transport of Oxygen and Carbon Dioxide in the Blood,” in *Medical Physiology*, ch. 28, pp. 654–668, Philadelphia, Pennsylvania: Elsevier Saunders, updated ed., 2005.
- [68] W. F. Boron and E. L. Boulpaep, “Control of Ventilation,” in *Medical Physiology*, pp. 712–734, Philadelphia, Pennsylvania: Elsevier Saunders, updated ed., 2005.
- [69] W. F. Boron and E. L. Boulpaep, “Acid-Base Physiology,” in *Medical Physiology*, ch. 27, pp. 633–653, Philadelphia, Pennsylvania: Elsevier Saunders, updated ed., 2005.

Appendix - Simulation model of the respiratory gas exchange

To create a better understanding in the (patho-)physiologic processes involved in the respiratory gas exchange (and subsequently the influence of PE on these processes), a simulation model was made using Mathworks Simulink. The model is based on several differential equations which will be elaborated in this chapter.

Gas exchange is a continuous process exclusively driven by passive diffusion. The amount of a gas which will cross the alveolar-capillary membrane per time unit is given by a simplified version of Ficks law:

$$\dot{V}_{net} = D_L(P_A - P_c) \quad (7.1)$$

in which \dot{V}_{net} denotes the amount of gas that will cross the alveolar capillary membrane per minute, D_L denotes the diffusion capacity for the lungs in mL (or mmol)/min/kPa, P_A denotes the partial pressure of the gas in the alveolar space and P_c denotes the partial pressure of the gas in the pulmonary capillaries. Using this equation, a model of the amount of gas present in the alveolar space ($V_{x,A}$) and capillaries ($V_{x,c}$) can be made.

$$\frac{dV_{x,A}}{dt} = -\dot{V}_{net} = -\frac{dV_{x,c}}{dt} \quad (7.2)$$

As the diffusion is dependent to the partial pressures of a gas in the alveolar space (and $P_x = \frac{V_x}{V_{total}}P_{total}$), the volume of the alveolar space is needed. Due to constant in- and expiration alveolar space is (assumed to) vary continuously dependent on the inspired or expired volume. As stated in equation 7.1, the amount of CO_2 diffusing from the capillaries in the alveoli is dependent on P_{A,CO_2} and P_{c,CO_2} . This partial pressure is caused by the amount of CO_2 dissolved in the blood. However, the total amount of CO_2 present in the blood is substantially larger than the amount of dissolved CO_2 as CO_2 also binds to hemoglobin. In figure 7.1, the relation between P_{CO_2} and the CO_2 content (the sum of the CO_2 bound to hemoglobin and the dissolved CO_2) per 100 mL blood is given. In physiological values for the CO_2 content, this relation is linear (as can be seen in the graph next to the blue arrow). For arterial blood this relation is given by eq 7.3, with P_{aCO_2} in kPa and C_{aCO_2} being the arterial CO_2 content in mL/dL.

$$P_{aCO_2} = \frac{C_{aCO_2} - 30}{0.45 * 7.5} \quad (7.3)$$

Due to the Haldane-effect, deoxygenated blood is able to carry more CO_2 compared to oxygenated blood. Therefore, the offset in the relation of the venous CO_2 content (C_{vCO_2}) and corresponding P_{CO_2} is somewhat larger. The resulting relation is given in eq 7.4.

$$P_{vCO_2} = \frac{C_{vCO_2} - 31.3}{0.45 * 7.5} \quad (7.4)$$

In figure 7.1, it can be seen that C_{vCO_2} is 4 mL/dL higher than C_{aCO_2} . This increase is caused by the CO_2 produced by metabolism. In rest the amount of CO_2 produced by metabolism equals

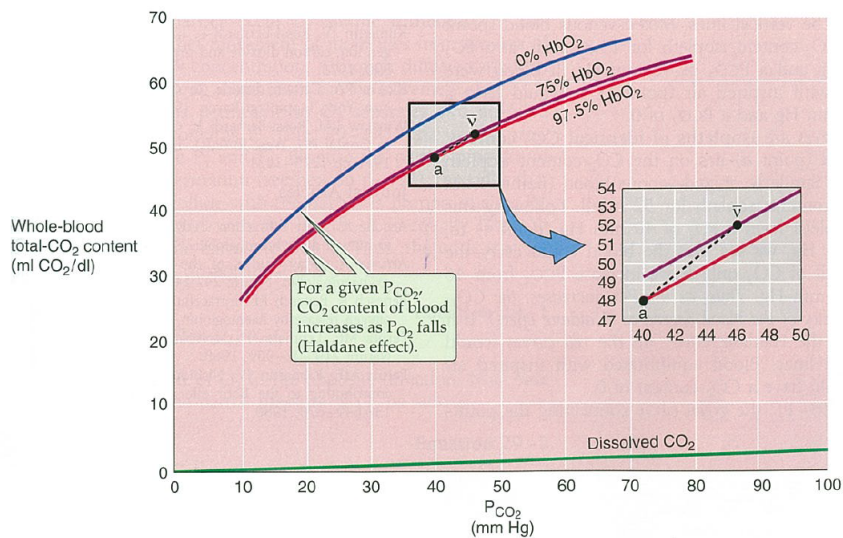


Figure 7.1: The CO_2 dissociation curve. Copied from Boron and Boulpaep [67]

about 240 mL/min. Assuming a blood volume of 6 L, this corresponds with the increase of $240/60 = 4$ mL/dL.

7.1 Respiratory control

As described earlier, the amount of CO_2 that diffuses from the capillaries into the alveoli is dependent on the relative amount of CO_2 already present in the alveoli (P_{A,CO_2}). With each ex- and inspiration, CO_2 rich air is exhaled and replaced by air containing practically no CO_2 , thereby diluting P_{A,CO_2} . To which extent the alveoli are ventilated (and thus how much CO_2 is exhaled) is regulated by a complex system of sensors and actuators. Though (in an awake setting) there is a basis ventilation independent of several aspects, the main parameter influencing minute ventilation is the P_{a,CO_2} . Chemosensors located on the surface of the medulla oblongata sense the pH in the cerebral spinal fluid (CSF). As hydrogen-ions cannot pass the blood-brain barrier and CO_2 can, the pH of the CSF is highly dependent on the P_{a,CO_2} . A high P_{a,CO_2} causes an increase in minute ventilation (thereby causing a decrease in P_{a,CO_2}). A low P_{a,CO_2} causes a decrease in minute ventilation (thereby increasing P_{a,CO_2}). Though the ventilatory drive is mainly determined by P_{a,CO_2} , changes in oxygen levels and pH can also influence minute ventilation. An overview of the

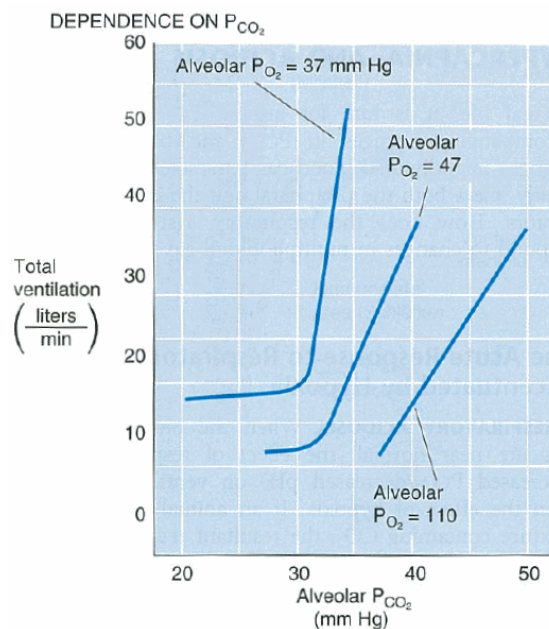


Figure 7.2: The ventilatory response to several levels of P_{a,CO_2} . Copied from Boron and Boulpaep [68]

classic J-shaped ventilatory response to several levels of P_{a,CO_2} is provided in figure 7.2. [68]

To model the ventilation, the inspired and expired flow is considered as a sine wave. The frequency of the sine is set to 60 divided by the respiratory rate. The amplitude (i.e. the peakflow) is set to that value that matches the desired tidal volume. The tidal volume is the integral of the flow signal of one half period (see equation 7.5) in which V_T denotes the tidal volume, t is the time, RR the respiratory rate and PF the peakflow. With a known RR and V_T , the needed peakflow can be calculated as stated below.

$$\begin{aligned}
V_T &= \int_0^{\frac{RR}{2}} PF \sin(2\pi \frac{RR}{60} t) \\
V_T &= -\frac{PF}{2\pi \frac{RR}{60}} \cos(2\pi \frac{RR}{60} \frac{RR}{2}) - (-\frac{PF}{2\pi \frac{RR}{60}} \cos(0)) \\
V_T &= 2 \frac{PF}{2\pi \frac{RR}{60}} \\
PF &= \pi \frac{RR}{60} V_T
\end{aligned} \tag{7.5}$$

The tidal volume and respiratory rate are determined by the desired respiratory minute volume. The change in respiratory minute volume is determined by the difference in actual P_{a,CO_2} with a reference P_{a,CO_2} which was set to 5.3 kPa. The initial minute ventilation was set to 6 L/min. Changes in respiratory minute volume were only made between respiratory cycles (i.e. when $t \frac{RR}{60} 2\pi$ equals a multiple of 2π).

Inspired air first flows through the conducting airways which was modeled as 20 compartments in series together consisting of 150 mL. Then, inspired air was divided over six alveolar compartment, each consisting of an end expiratory volume of 400 mL. Flow to all compartments was set to 1/6 of the total flow reaching the alveolar space.

7.2 Bicarbonate buffer

Though in a normal physiological state the amount of exhaled CO_2 approximately equals the amount of CO_2 produced by metabolism (i.e. there is an equilibrium), a disequilibrium does not necessarily result in an in- or decrease of P_{a,CO_2} . This is caused by the bicarbonate (HCO_3^-) buffer, depicted in equation 7.6.



An increase in CO_2 results in a right shift of the buffer, and will thus increase the amount of H^+ (and therefore lowers pH, creating an acidosis) and HCO_3^- . Vice versa, a decrease in CO_2 results in a shift to the left part of the equation, and will thus decrease the amount of H^+ (increasing pH, creating an alkalosis) and HCO_3^- . The buffer is in equilibrium when a certain combination of the concentrations of its components equal the equilibrium constant K as depicted in equation 7.7. [69]

$$K = \frac{[HCO_3^-][H^+]}{[H_2CO_3]} = 8.05 * 10^{-4} mmol/L \tag{7.7}$$

The concentration of H_2CO_3 is dependent on the solubility of CO_2 in water (k_{aq} , 0.225 mmol/L/kPa). Therefore $[H_2CO_3] = k_{aq} P_{CO_2} = 0.225 P_{CO_2}$ yields. The essence of the buffer is that it tries to seek an equilibrium where equation 7.7 applies. Therefore, the change of $[HCO_3^-]$, $[H^+]$ and H_2CO_3 over time due to the buffer changes can be described by equation 7.8 where K is the actual value of

K , K_{ref} is $8.05 \cdot 10^{-4}$ mmol/L and S is a theoretical constant providing a measure for the reaction speed.

$$\begin{bmatrix} \frac{[HCO_3^-]}{dt} \\ [H^+] \\ \frac{[H_2CO_3^-]}{dt} \end{bmatrix} = S(K - K_{ref}) \begin{bmatrix} -1 \\ -1 \\ 1 \end{bmatrix} \quad (7.8)$$

7.3 Simulation

At each time step, the total amount of CO_2 present in each region was calculated. By combining flow data and the P_{CO_2} in the first compartment of the conducting airways (which can be considered as the expired P_{CO_2}), volumetric capnograms were constructed. Blood flow to each alveolar compartment was initially set to 1/6 of the total blood flow to the lungs which remained constant during the entire simulation. A constant shunt fraction of 5% (i.e. blood that does not pass the alveolar space) was also incorporated in the simulation. Pulmonary embolism was simulated by decreasing the blood flow to one compartment (and dividing the remainder over the healthy compartments). A GUI was made to enable easy use of the model. A simulation of 1200 seconds was performed where blood flow to three of the six compartments was obstructed at $t=600$. After a normalization period (see figure 7.3), 12.1 breaths with a volume of 505 mL were taken to maintain P_{a,CO_2} at 5.3 kPa. Exhaled CO_2 was 235 mL/min. Analysis of the volumetric capnogram showed an PET_{CO_2} of 5.26 kPa, a slope of phase III of the volumetric capnogram of 0.53 kPa/L, anatomic dead space was calculated to be 146.9 mL, VD_{aw}/VT was 29.1%. Bohr's dead space is 0.0 mL (VD_{Bohr}/VT also 0%). These values are comparable with values reported from healthy subjects in literature. The calculated anatomic dead space (146.9 mL) is a very good approximation of the modeled anatomic dead space (150 mL). After the introduction of the diminished blood flow to three of the alveolar compartments, a new initialization period takes place. After initialization (see figure 7.4), 15.9 breaths with a volume of 749 mL were taken to maintain P_{a,CO_2} at 5.3 kPa. Exhaled CO_2 was 281 mL/min. Analysis of the volumetric capnogram showed an PET_{CO_2} of 2.87 kPa, a slope of phase III of the volumetric capnogram of 0.27 kPa/L, anatomic dead space was calculated to be 145.3 mL, VD_{aw}/VT was 19.4%. Bohr's dead space was 345.1 mL (VD_{Bohr}/VT 46%). Most of the volumetric capnogram parameters are half the value they were in the normal situation, which can be expected with half of the pulmonary vasculature blocked. However, it was expected that VCO_2 remains constant (and not slightly increases). A possibility is that the normalization period had not ended completely. It can be noted that the calculated VD_{aw} slightly differs from its value in the healthy situation but is still a good representation of its true value. The calculated Bohr's dead space (46%) is a good representation of the true dead space ventilation (50%). It can be noted that the extra effort needed to normalize P_{a,CO_2} when half of the pulmonary vasculature is blocked is not very high (50% increase in tidal volume, 33% increase in respiratory rate).

7.4 Limitations

In the simulation no cardiovascular changes are made after obstruction of the pulmonary vasculature. In reality, pulmonary artery pressure will increase significantly eventually diminishing cardiac output and thus causing death. This was not implemented in the model for two reasons. First, the model was chosen to keep as simple as possible for computational reasons (calculations were performed at a personal laptop with limited calculation power). Second, the lack of cardiovascular response allows for the simulation of an extreme obstruction percentage clarifying the influence of the obstruction on respiratory gas exchange.

Another limitation is that all alveolar compartments empty simultaneously and there is instantaneous mixing. In reality this does not happen. This can cause $VDaw$ to be increased in PE if the affected alveoli empty at the first part of exhalation. Finally, hypocapnic bronchoconstriction was not modeled.

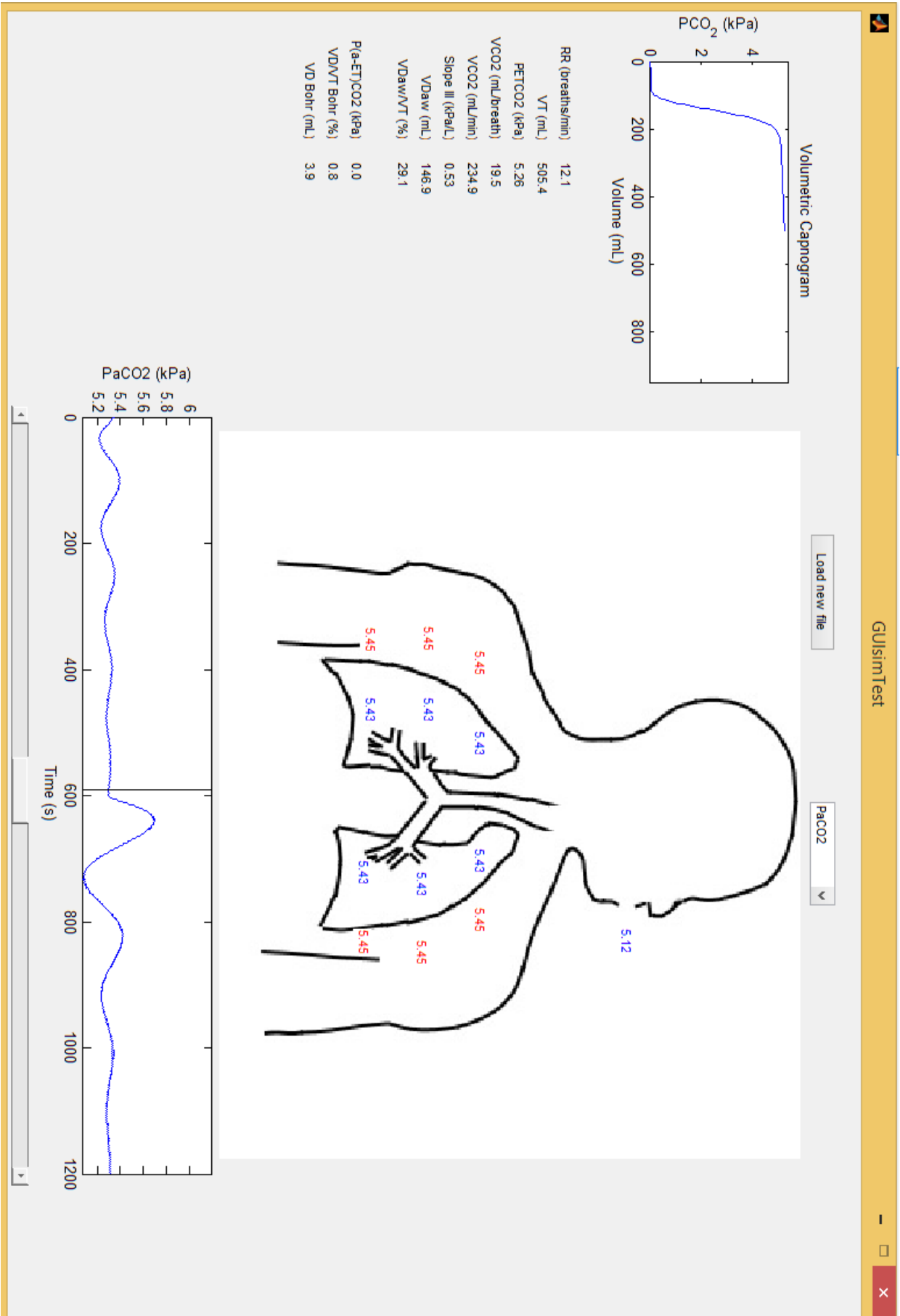


Figure 7.3: Results of the simulation at the end of normalization of the healthy situation. Blue numbers indicate PCO_2 in air, red numbers PCO_2 in blood.

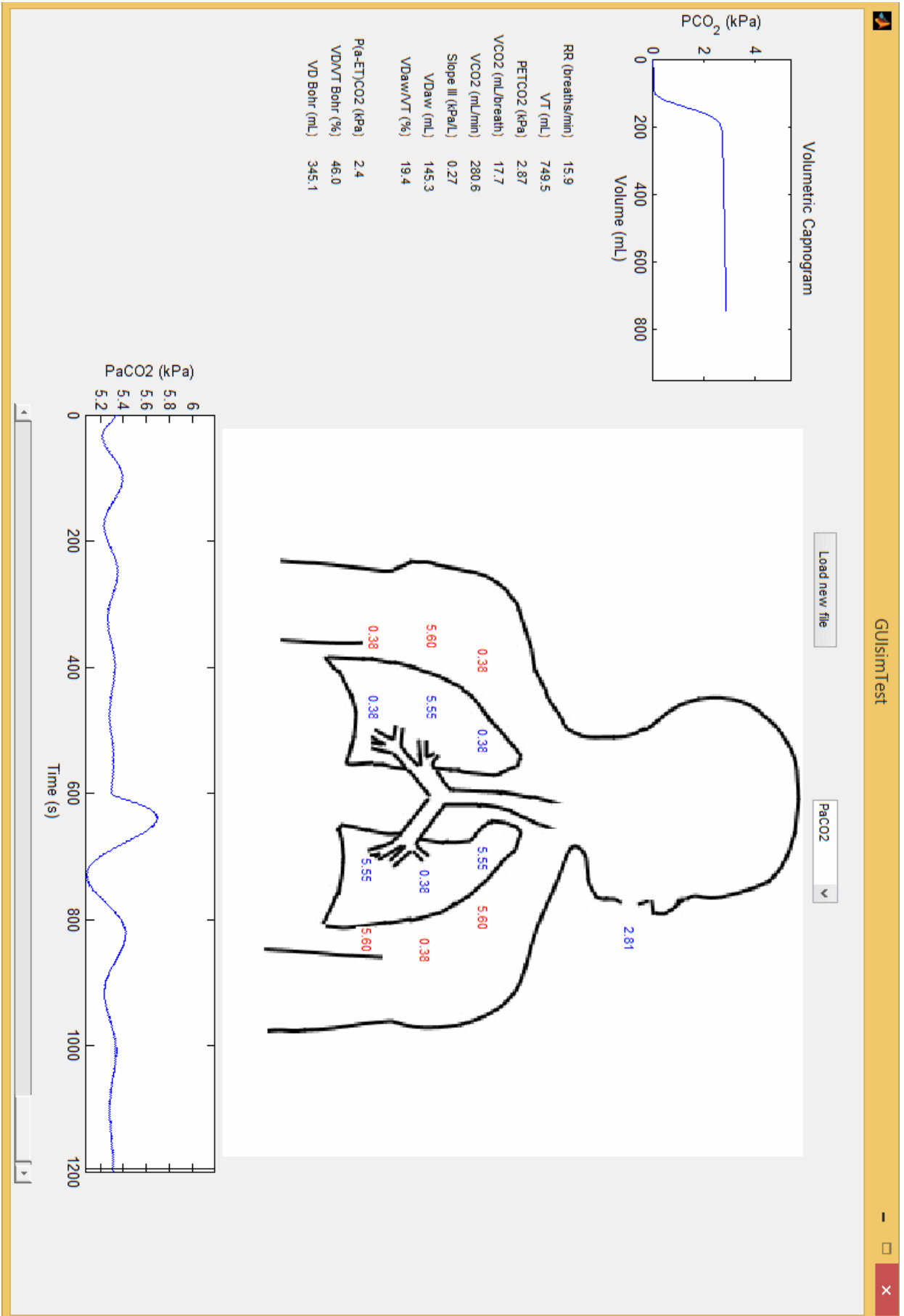


Figure 7.4: Results of the simulation at the end of normalization after obstruction of blood flow to three of the six alveolar compartments. Blue numbers indicate P_{CO_2} in air, red numbers P_{CO_2} in blood.